Cloning, *in silico* characterization and phylogenetic analysis of the NMDA receptor in crucian carp

Cand. Scient. Thesis by Dag Are Steenhoff Hov

Supervisors:
Göran E. Nilsson
Stian Ellefsen

Programme for Physiology
Department of Molecular Biosciences
Faculty of mathematics and natural sciences
UNIVERSITY OF OSLO

Acknowledgements

Lykken er et hovedfag!

Aller først vil jeg si tusen takk til min hovedveileder, Göran, for at du aldri helt ga opp håpet. Jeg er takknemlig for at du fikk tid til å lese gjennom oppgaven. Du er en kunnskapsrik, lun og god person og med ditt om noe svenske, men inkluderende vesen har jeg alltid følt at det var greit med én øl til. Takk for du har gjort alle i utgangspunktet faglige Klubban- og vintermøter og Drøbak-kurs til festlige affærer med spontane innfall av nakenbading og badstu. Det er alltid like trivelig å kore deg gjennom 'Wild Rover'! Soppturer med påfølgende gourmet-tango på kjøkkenet ditt forblir uforglemmelige.

Min medveileder, gode kamerat og molekylærbiologiske støtte(s)pi(l)lar, Stian, som gjerne er tre ønsker på en gang: En overraskende morsom og leken kar som liker sjokoladeis. Skrive kan han også. Takk for det du har lært meg og tida du har brukt på meg. Dette er bare begynnelsen.

Det sies at man ikke kan velge sine foreldre. Slik kjennes det litt med gruppa vår også. Det måtte bli fysiologi og den litt egenrådige og nokså fanoksiske karpefisken karuss. Hyggelige mennesker, kake- og pubmøter tror jeg har bidratt vel så mye til min trivsel. Takk til alle sammen.

Også takk til lunsjgjenger med Guro som samlingspunkt. Hold ut, Guro! Takk, Helene, for at du tok deg tid til å lese korrektur helt på tampen. Stine bør også få navnet sitt på trykk for at hun tar meg med på skumle ting én gang i året. Kristine synger, baker og kan også noen lure triks i Word, takk for hjelp! Takk til Miriam og Kjetil og resten av studentene her inne som også gjør bukhulen vår så trivelig!

Ellers takk til alle på avdelinga som har vært med på å gjøre tiden min her som hovedfagsstudent så bra. På program for generell fysiologi har vi høy tetthet av kunnskap, julebord, hytteturer og vårfester og jeg kan bare være fornøyd for å ha valgt meg hit.

Takk til familien min som har støttet meg og ventet i spenning, fra rundt 1250 km lenger nord og omtrent 50 km lenger sør. Og takk til pappa som har gjort en kjempejobb med å være pappa helt oppe fra Lofoten.

Min kjære, søte, tolmodige Kristin. Nå er det over! ☺ Etter at du fant meg og jeg fant deg og vi fant oss en leilighet sammen, har det nok blitt lettere å leve litt mer vanlig. Akkurat nok mer vanlig til å bli ferdig med et hovedfag. Men ikke mer vanlig enn at vi kan dra på tur til fine steder og dykke litt og se på fine fisker eller gå opp på et fjell og se på fin utsikt, når det passer seg sånn. Takk for at du holder ut med meg! ☺ Nå kommer jeg hjem til deg og tomatene våre på Teisen! Nå blir det du og jeg!

Oslo, den 29. juni 2007

Abstract

The crucian carp survives anoxia with the brain turned on. In such a state it is crucial to lower energy expenditures. This can be achieved by lowering the permeability of ionotropic receptors such as the N-metyl-D-aspartate receptor (NMDAR). We hypothesized that the crucian carp NMDAR possess properties important for anoxic tolerance. This thesis reports the full-length cloning of the NR1 subunit, as well as ESTs for NR2A-D and NR3A in crucian carp. Phylogenetic analyses supported the identity of all subunits, and suggested the finding of two closely related paralogs for NR1, NR2A and NR2D. These paralogs provide evidence for a recent genomic duplication event in the crucian carp lineage. Protein analyses of NR1 revealed no obvious adaptations important for anoxic survival. All key properties were conserved. However, a novel splice cassette, 'NTSG', was found in the N-terminal. This was predicted to represent a functional N-glycosylation site. Real-time RT PCR primers were designed for assessments of gene expression.

Abbreviations

aa	Amino acid
al	*Apteronotus leptorhynchus* (knifefish)
AMPA	alpha-amino-3-hydroxy-5-methyl-4-isoazolepropionic acid
ap	*Anas platyrhynchos* (duck)
ATP	Adenosine Triphosphate
BLAST	Basic Local Alignment Search Tool
bp	Base pairs
C1	C-terminal alternative splice cassette in NMDAR subunit NR1, 37 aa
C1'	C-terminal alternative splice cassette in NMDAR subunit NR1, 19 aa
C1''	C-terminal alternative splice cassette in NMDAR subunit NR1, 9 aa
C2	C-terminal alternative splice cassette in NMDAR subunit NR1, 38 aa
C2'	C-terminal alternative splice cassette in NMDAR subunit NR1, 22 aa
cc	*Carassius carassius* (crucian carp)
cDNA	Complementary DNA
CDS	Coding Domain Sequence
CNS	Central Nervous System
dr	*Danio rerio* (zebrafish)
ER	Endoplasmatic Reticulum
EST	Expressed Sequence Tag
gg	*Gallus gallus* (chicken)
GSP	Gene Specific Primer
hpf	Hours postfertilization
hs	*Homo sapiens* (human)
mm	*Mus musculus* (mouse)
N1	N-terminal alternative splice cassette in NMDAR subunit NR1, 21 aa
NMDA	N-metyl-D-aspartate
OD	Optical Density
RACE	Rapid Amplification of cDNA Ends
rn	*Rattus norvegicus* (rat)
rRNA	Ribosomal RNA
RT PCR	Reverse Transcriptase Polymerase Chain Reaction
TM	Trans Membrane
tn	*Tetraodon nigroviridis* (spotted green pufferfish)
tr	*Takifugu rubripes* (japanese pufferfish)
ts	*Trachemys scripta* (red-eared slider turtle)
WGD	Whole Genome Duplications
xl	*Xenopus laevis* (African clawed frog)

Table of Contents

1 Introduction

Vertebrates depend on oxygen to survive, and most species will experience cell death after minutes of anoxia. Brain tissue is particularly sensitive and vast resources are put into finding ways to minimize damage caused by oxygen loss. Notably, this challenge has already been solved by nature. Several vertebrate species have evolved ways to survive hours and months without oxygen. Examples are the epaulette shark (*Hemiscyllium ocellatum*), the frogs (*Rana sp*), several species of freshwater turtles (genus' *Chrysemys* and *Trachemys*) and cyprinid fish of the genera *Carassius* (goldfish, *Carassius auratus*; crucian carp, *Carassius carassius*). Some of these species, like red-eared slider turtle (*Trachemys scripta*) and crucian carp, survive anoxia for months at temperatures close to 0 °C. While the turtle enters a comatose state, the crucian carp stays conscious and somewhat mobile (Lutz et al., 2003).

1.1 The Problem of Anoxia

In animals, a lack of oxygen will halt mitochondrial electron transport, whereupon glycolysis will be the only route for ATP production. This reduces ATP yield obtained per mole glucose from 36 moles to 2 moles, resulting in ATP demands exceeding ATP production, and eventually ATP-depletion. In turn, this impedes all energy demanding processes, such as ion-pumping through the Na^+- K^+-ATPase. In normoxia, this particular ATPase maintains the membrane potential by sending Na^+-ions out of the cell and K^+-ions into the cell. When this function is halted during anoxia, K^+ accumulates in the extracellular fluid, eventually leading to depolarization of cells such as neurons. This involves movement of Ca^{2+} and Na^+ down their electrochemical gradient into the neurons. In the brain, this process will result in release of neurotransmitters, such as glutamate, further increasing the rate of depolarization. The increasing cytoplasmic calcium concentration will set off a number of cellular processes that kills the cell. For review on ischemic cell death in neurons, see Lipton (1999).

Glutamate is the main excitatory neurotransmitter in vertebrate central nervous systems (CNS). It is known to activate ionotropic receptors such as the N-methyl-D-aspartate

(NMDA) receptor. Excessive amounts of extracellular glutamate have been shown to result in neurotoxic events. This has been proposed to be mainly effected by prolonged opening of NMDARs and the resulting inlet of Ca^{2+} (Szatkowski and Attwell, 1994). Further details on the NMDAR will be given later.

1.2 The Anoxia Tolerant Crucian Carp Solves the Problem

The crucian carp is a fresh water fish that lives in lakes as well as small and shallow ponds in North Europe. During winter these ponds are covered by thick layers of ice and snow, blocking out oxygen and sunlight. Thus, no new oxygen will diffuse into the water and no photosynthetic activity will occur. The result is often a depletion of the dissolved oxygen and an anoxic environment. There are two strategies that can promote survival in such an environment. The first is to up-regulate glycolysis and increase the consumption of glucose. This has been shown to occur in crucian carp, which up-regulates key glycolytic enzymes like fructose 2.6-bisphosphate (Storey, 1987). The second strategy is to lower the energy expenditure, and meet the reduced rate of ATP production. The crucian carp has been shown to do so in several ways, such as by reducing swimming activity by 25-50 % (Nilsson et al., 1993), and by becoming completely blind (Johansson et al., 1997). However, when vertebrates manage to balance anoxic energy consumption with anoxic energy production, they are faced with yet another problem: acidification. The end-product of glycolysis is lactate, and plasma levels of this acid, along with H^+, will rapidly increase to lethal levels unless it is eliminated. Crucian carp has evolved a peculiar solution to this problem. It transforms lactate, via pyruvate and acetaldehyde, into ethanol that can diffuse across the gill surface into the ambient water (Johnston and Bernard, 1983). This mechanism is also found in the bitterling (*Rhodeus amareus*) (Wissing and Zebe, 1988) and in the closely related goldfish (Shoubridge and Hochachka, 1980). For an overview, see Figure 1. Freshwater turtles have evolved a very different strategy. They do not get rid of their lactate, but they buffer its detrimental effects with their Ca_2CO_3-containing shells (Jackson, 2000). Hence, their blood is essentially limed.

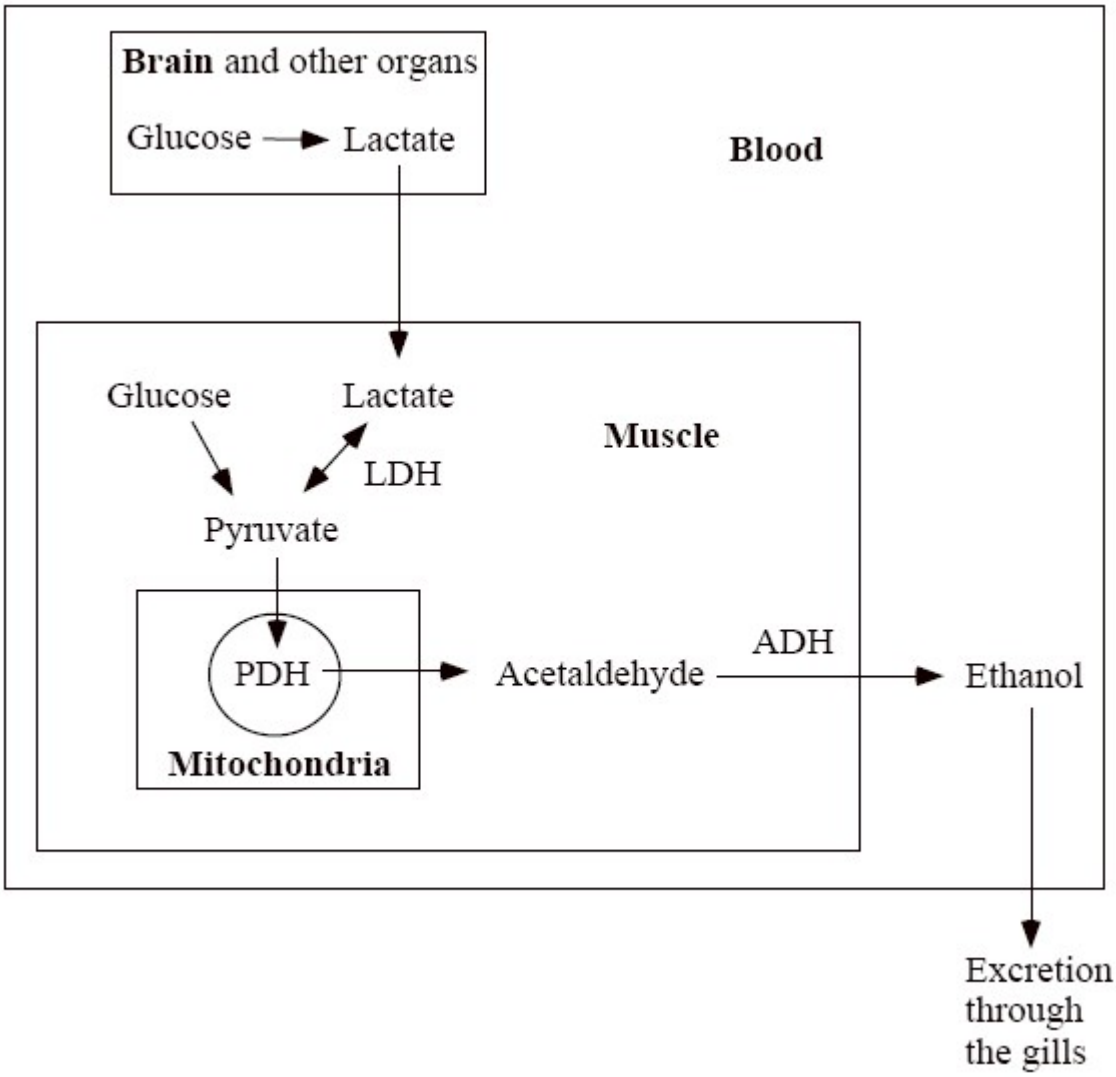

Figure 1. Ethanol-producing pathway in the genus *Carassius*. By releasing ethanol into the water, crucian carp and goldfish avoid a build-up of anaerobic end-product. LDH, lactate dehydrogenase; ADH, alcohol dehydrogenase; PDH, pyruvate dehydrogenase. (from Lutz and Nilsson, 1997)

In the end, the size of the glycogen store seems to be the factor that limits anoxic survival in crucian carp (Nilsson, 1990). Indeed, its liver has the largest glycogen content measured in a vertebrate, constituting up to 25-30 % of the liver wet weight (Hyvärinen et al., 1985).

1.3 The NMDA Receptor

Since the discovery of glutamate's ability to excite spinal neurons in domesticated cat (Curtis et al., 1959), there has been extensive efforts to characterize the nature of glutamate receptors (for review, see Chen and Wyllie, 2006; Cull-Candy et al., 2001; Cull-Candy and Leszkiewicz, 2004; Dingledine et al., 1999; Hollmann and Heinemann, 1994). The glutamate receptors divide into two main categories, the metabotropic and the ionotropic. Metabotropic glutamate receptors mediate their signal via G-proteins and other intracellular signaling pathways. They have several functions and are important modulators of ionotropic glutamate receptors (for review see Conn and Pin (1997)). The ionotropic glutamate receptors open an ion channel that gates Ca^{2+} and/or Na^{+} into the neuron and excites the cell. Intracellular Ca^{2+} will bind various components of the cell to modify synapse behaviour and plasticity. Ionotropic glutamate receptors are divided into three groups based on specific agonists that bind and open the channels: NMDA receptors, alpha-amino-3-hydroxy-5-methyl-4-isoazolepropionic acid (AMPA) receptors and 2-carboxy-3-carboxymethyl-4-isopropenylpyrrolidine (kainate) receptors.

The NMDAR has been ascribed an important role in long term potentiation (LTP) (Nicoll, 2003) and neurotoxicity (Szatkowski and Attwell, 1994) and has been particularly well studied. It has a quite complex action, and its opening requires coincident binding of glutamate and glycine, as well as depolarization of the membrane. The latter is important to remove a Mg^{2+} residue that blocks the ion pore at resting potential. In addition, the receptor is modulated by Zn^{2+}, polyamines, H^{+} and other extra- and intracellular factors as described in several reviews (Cull-Candy et al., 2001; Dingledine et al., 1999; Hollmann and Heinemann, 1994).

The NMDAR gene family consists of three sub-families; NR1, NR2 and NR3. Functional NMDARs are made up of two NR1 subunits and two NR2 subunits (Cull-Candy et al., 2001), which are thus believed to have a tetrameric structure (Premkumar and Auerbach, 1997). The NR3 have been reported to co-occur with functional NR1/NR2 receptors, probably instead of one of the NR2 subunits (Al-Hallaq et al., 2002). The first member of the NMDAR gene family, NR1, was cloned in 1991-1992 in mouse

and rat and was found to consist of one subunit (Moriyoshi et al., 1991; Yamazaki et al., 1992). NR1 diversity is still possible through alternative splicing of exons 5 (extracellular N-terminal), 21 and 22 (intracellular C-terminal), giving a total of 8 functional splice variants (McBain and Mayer, 1994). These splice variants give NMDARs with different structural, physiological and pharmacological properties (Zukin and Bennett, 1995). The NR2 sub-family was cloned in 1992-1993 in mouse and rat and consist of four subunits; NR2A (Meguro et al., 1992; Monyer et al., 1992), NR2B (Kutsuwada et al., 1992; Monyer et al., 1992), NR2C (Kutsuwada et al., 1992; Monyer et al., 1992) and NR2D (Ikeda et al., 1992; Ishii et al., 1993). The NR2 subunits share only 15-20 % homology with NR1, but are highly homologous (50-70 %) to each other (Ishii et al., 1993). All NR2 subunits except NR2A have splice variants. The NR3 sub-family was cloned in the years 1995-2002 in mouse, rat and human and consists of two subunits; NR3A, (Andersson et al., 2001; Ciabarra et al., 1995; Sucher et al., 1995) and NR3B (Andersson et al., 2001; Chatterton et al., 2002; Nishi et al., 2001). The NR3 subunits share approximately 50 % amino acid identity and around 27 % with NR1 and NR2 subunits (Ciabarra et al., 1995).

The two NR2 subunits present in functional NMDARs can exist either as homodimers or heterodimers. While NR1 subunits possess the glycine binding site, NR2 subunits possess the glutamate binding site. The properties of NMDARs are largely dependent upon the NR2 composition. Receptors comprising NR1/NR2A and NR1/NR2B have high Ca^{2+} conductance with a high sensitivity to block by Mg^{2+}, whereas receptors comprising NR1/NR2C and NR1/NR2D have low Ca^{2+} conductance with a lower sensitivity to extracellular Mg^{2+}. The time from channel opening to channel closing (deactivation time) is depending on what NR2 subunit present in the receptor and spans from milliseconds with NR2A included, to minutes caused by the NR2D subunit. The inclusion of the NR2B or NR2C subunits results in about the same deactivation time which is a bit longer than that of NR2A (Dingledine et al., 1999). The different NR2 subunits show different levels of expression in rat brain, with the following expression profile in adult rat brain tissue; NR2B > NR2A > NR2D = NR2C (Goebel and Poosch, 1999) (See also Figure 11). The relative occurrence of NR2 subunits is not rigid and

changes during an organism's development. The NR2D is expressed prenatally mainly in the midbrain and reaches a peak at postnatal day 7 and from there decreases until adult levels. These types of changes has been observed to alter the properties of NMDARs, such as conductance, deactivation kinetics and the strength of Mg^{2+} block (Monyer et al., 1994).

NR3A and NR3B possess putative glycine binding sites that are similar to that of NR1 (Chatterton et al., 2002). Still, their functional role in NMDAR biology is unclear. However, some cues have been found to suggest a role. Firstly, they form excitatory glycine receptors when co-expressed with NR1 in *Xenopus* oocytes. These receptors can not be biologically abundant, and they do not react to glutamate or NMDA. They are permeable to cations, except Ca^{2+}, and do not possess a Mg^{2+} block (Chatterton et al., 2002). Secondly, NR3 has been reported to influence the number of NMDARs found on the neuron surface and also decrease Ca^{2+} permeability of NR1/NR2 receptors (Perez-Otano et al., 2001). Additionally, co-immunoprecipitation studies suggest that NR1, NR2 and NR3 subunits exist as receptor complexes (Al-Hallaq et al., 2002). Thus, NR3 subunits may play a role in the modulation of functional NMDARs.

The NMDAR subunits have more or less the same structure as the other ionotropic glutamate receptors (review by McFeeters and Oswald, 2004). They have an extracellular N-terminal domain, followed by an S1 segment that takes part in the ligand binding domain. They also have a transmembrane (TM) segment, TM1, preceding the pore-forming P-element. The P-element enters the membrane from the cytosolic side, makes a turn within the membrane and returns to cytosol. After a subsequent TM segment TM3, an extracellular domain makes up the remainder of the ligand binding domain, the S2 segment. This part of the protein enters the membrane from the outside and becomes TM4, before it ends in a large intracellular C-terminal domain. The overall structure of the NR1 subunit is more or less the same between knifefish (*Apteronotus leptorhynchus*) and rat, and only the C-terminal domain shows significant differences, especially when it comes to alternative splicing. The nomenclature used for the alternative splice cassettes and TM regions in this thesis are summarized in Figure 2.

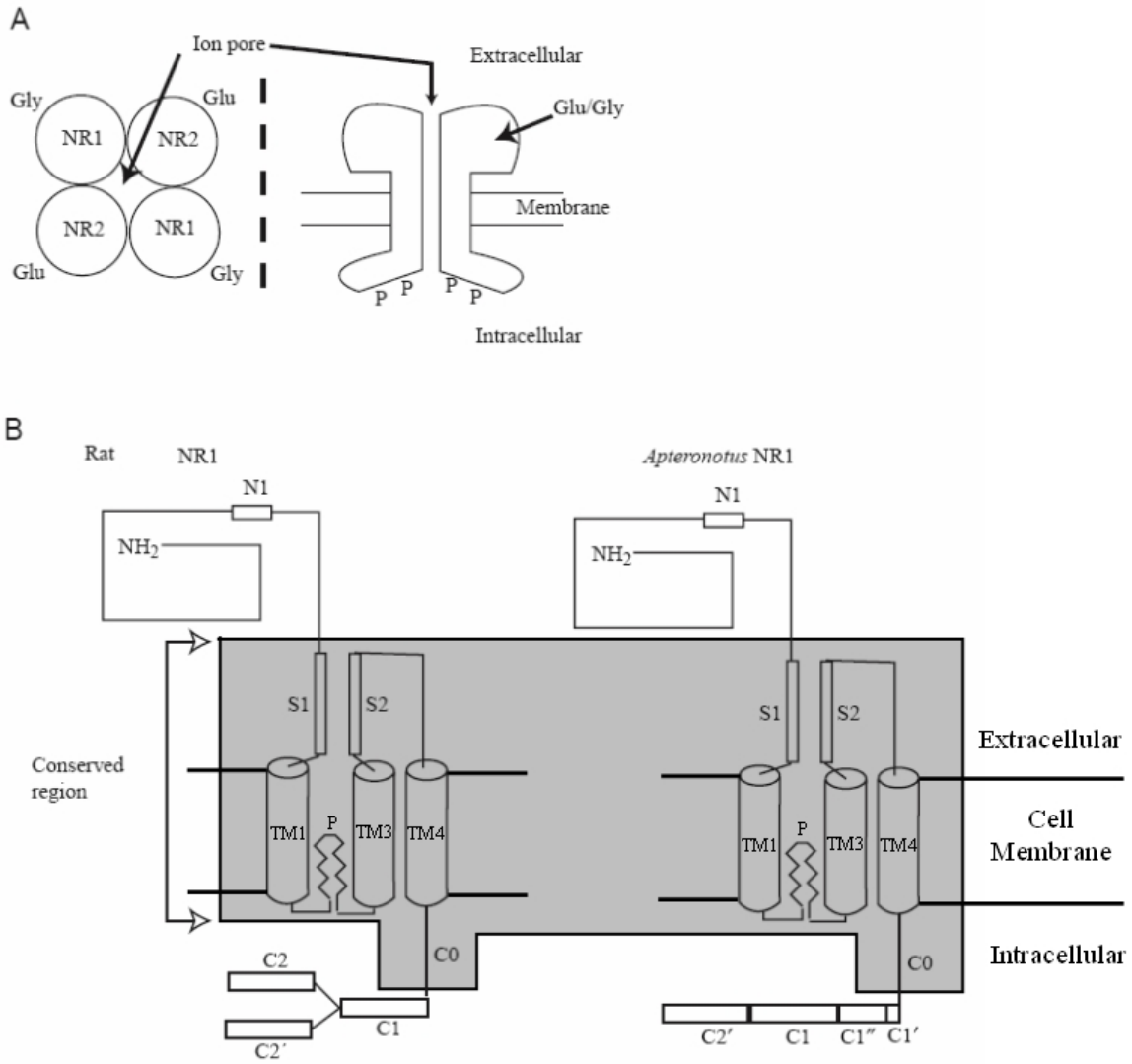

Figure 2. Structure of the N-methyl-D-aspartate (NMDA) receptor complex. (A) The NMDA receptor contains four subunits, two NR1 and two NR2 subunits. The ion conduction pore lies in the center of the complex. Glu, glutamate; Gly, glycine; P, phosphate. (B) The proposed secondary structures for NR1 from rat and *Apteronotus leptorhynchus*. The shaded area includes the regions in which the amino acid sequences are nearly identical. The boxed segments labeled *N1*, *C1*, *C1'*, *C1''*, *C2* and *C2'* indicate the positions of alternatively spliced cassettes. The boxed segments *S1* and *S2* indicate the ligand binding domains. Segment *C0* is highly conserved. (modified from Dunn et al., 1999)

The presence of the NR1 N1 splice cassette (mammalian exon 5) has been reported in teleost (Bottai et al., 1998; Cox et al., 2005; Tzeng et al., 2007). This cassette creates an external loop that consists of positively charged residues. This loop will change the NR1 structure and sterically hinder the potentiating effects of polyamines and the inhibitory effects of protons (Traynelis et al., 1995; Zheng et al., 1994). The C0 cassette (exon 20) seems to be expressed in all functional NR1 splice variant (Dingledine et al., 1999) and

comprise a binding site for calmodulin. In the presence of Ca^{2+}, calmodulin has been found to desensitize NMDARs (Ehlers et al., 1996). The C1 cassette (exon 21) is often included as a part of teleost NR1 transcripts. This is also case for the teleost specific C1' and C1'' cassettes. Further, the C2 cassette (5' portion of mammalian exon 22) has not been reported to be expressed in teleost NR1, but the C2' cassette (alternative stop codon of mammalian exon 22) seems to be present in all teleost NR1 variants (Bottai et al., 1998; Cox et al., 2005; Tzeng et al., 2007).

In mammals, the most commonly expressed NR1 splice variants include both the C1 and the C2 cassette. A large pool of this variant has been found intracellularly, presumably in the endoplasmatic reticulum (ER) (Chazot and Stephenson, 1997). C1 contains an ER retention signal (RXR, where X can not be an acidic amino acid). However, this signal can be masked by NR2 subunits or by postsynaptic density (PSD) family proteins. PSD proteins bind to the PDZ domain 'STVV', which is found on the C2' cassette. Splice variants expressing the C2' cassette or lacking the C1 cassette, are able to leave the ER and reach the cell surface without binding to NR2 subunits. For review on early events in glutamate receptor trafficking, see Vandenberghe and Bredt (2004).
Studies of the anoxia tolerance of western painted turtles (*Chrysemys picta*),have revealed that the opening probability of NMDARs is reduced by 65 % after one hour of anoxia (Buck and Bickler, 1998). Without this reduction, anoxic turtle neurons will die within hours. Further, NMDAR surface expression has been shown to be lowered in western painted turtles after 3-21 days in anoxia (Bickler et al., 2000).

1.4 Anoxia Tolerance in Fish – Evolutionary Perspective

Fish share a common ancestor with all vertebrates. Studies have shown that two whole genome duplications (WGDs) probably occurred early in vertebrate evolution. The organisms in a diploid (2N) population then doubles their number of similar chromosomes, tetraploidization (4N), creating a copy set of every gene (paralogs), and slowly returns to the state of diploidy, rediploidization. The resulting increase in the number of genes from the WGDs made the advanced body form of vertebrates possible (Sidow, 1996). Indeed, there has been proposed to be a direct relationship between gene

copy number and species diversity (Amores et al., 1998). Further, the evolutionary time span from non-vertebrates, such as cephalochordate amphioxus (*Amphioxus lanceolatus*), to the more complex vertebrates, such as cartilaginous fish, is relatively short and supports the positive effect of a possible WGD (see Figure 3).

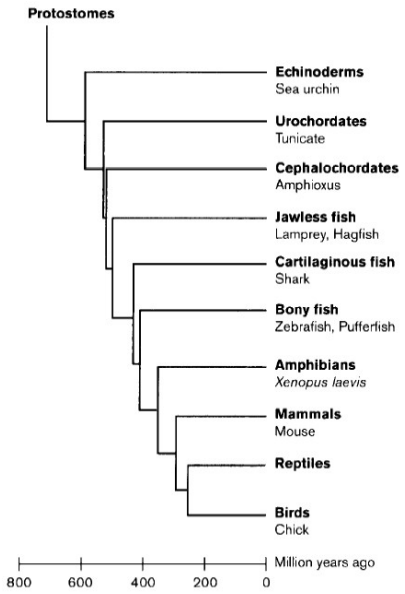

Figure 3. Phylogenetic relationships among extant deuterostome classes and phyla. (The exact branching order of lampreys and hagfish is a matter of debate.) Note that the time span in which the advanced vertebrate body plan evolved - between the divergence of amphioxus and cartilaginous fish - is relatively short. Known phylogenies such as this one are essential for inferring duplications in gene families and other evolutionary events. (from Sidow, 1996)

Yet another WGD event has been reported early in the ray-finned fish lineage after the divergence from tetrapods (the 1-2-4-8 hypothesis, Figure 4) (Meyer and Schartl, 1999). This suggestion is supported by the presence of hundreds of duplicated genes in pufferfishes (*Takifugu rubripes, Tetraodon nigroviridis*) and zebrafish (*Danio rerio*). These genes have been reported to be co-orthologous to single-copy tetrapod genes (Taylor et al., 2003). Analyses of sequence divergence between these paralogs suggests that these genes were duplicated between 300-450 million years ago (Taylor et al., 2001). This duplication is proposed to have happened after the divergence of sturgeons and may have given the species-richness of the teleost lineage. This is an extremely diverse group of vertebrates, and with more than 23500 species, the ray-finned fishes represent more

than 95 % of all living fish species and about 50 % of all extant vertebrate species. More than 99.8 % of ray-finned fishes belong to the teleosts. Examples of non-teleost ray-finned fishes are the bichirs and sturgeons (Figure 4) (for review on biodiversity in teleost fish, see Volff, 2005). Many teleost lineages, like the atlantic salmon (*Salmo salar*) and rainbow trout (*Oncorhynchus mykiss*) or the genus *Carassius* (crucian carp and goldfish), have experienced yet another WGD leading to an even more complex genomic arrangement (Leggatt and Iwama, 2003). Organisms in the genus Carassius are today indeed found to be tetraploids (Raicu et al., 1981).

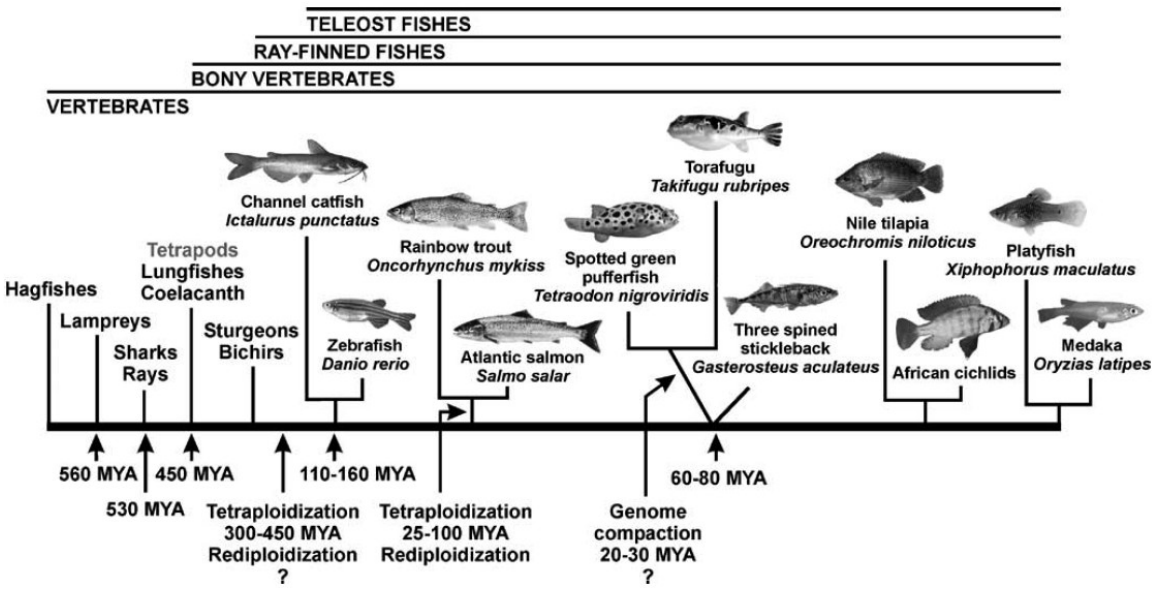

Figure 4. The fish lineage. Origin of fish pictures: Manfred Schartl and Christoph Winkler (medaka, zebrafish, platyfish and *Tetraodon*), Erwin Schraml (African cichlid), John F Scarola (rainbow trout and Atlantic salmon), Suzanne L and Joseph T Collins (channel catfish), Bernd Ueberschaer (Nile tilapia), Konrad Schmidt (three spined stickleback) and Greg Elgar (Torafugu). (from Volff, 2005)

Force et al. (1999) the duplication-degeneration-complementation (DDC) model to explain the fates of duplicated genes. The model defines three potential courses of events; (i) mutations in regulatory elements prevents gene copies from being expressed, and they end up as a pseudogenes (nonfunctionalization), (ii) degenerative mutations occur in one copy of a gene, but not in the other, and make both copies necessary to preserve ancestral functions (subfunctionalization) and (iii) positive mutation creates new functions in one copy of a gene, and gives preservation of the functions of the non-

mutated copy to retain ancestral functions (neofunctionalization). Further, the model of conservation of paralogs by dosage effect is presented. If higher survival rates are obtained by increasing the number of gene copies of a specific gene, then both paralogs resulting from a duplication will be preserved.

Water holds much less oxygen than air (10 ml/L water compared to 210 ml/L air at 0 °C) and the diffusion rate in water is only 1/10000 of that in air. As a result, oxygen may be rapidly depleted in water and new oxygen will only slowly return. This makes fish likely to experience hypoxia in their habitats, especially in stagnant waters with high degrees of biomass and little supply of photons. Thus, aquatic habitats will often favour organisms possessing features to handle periods of decreased oxygen supply. Several examples of this can be mentioned. The crucian carp lives in small ponds that may become anoxic during winter time, when ice and snow blocks oxygen synthesis/access. The epaulette shark is a marine example of fish that has adapted to severe hypoxia occurring at shallow coral reef platforms. The low tide at night brings oxygen levels down to 20 % due to the respiration of coral and coral-living organisms (Nilsson and Renshaw, 2004). Also, the Amazon water bodies become hypoxic and even anoxic in periods of the year, whereupon many species have been found to change morphology and metabolism to meet the challenge (Val et al., 1998).

1.5 Aim

Due to its high energy demands, the brain is possibly the most anoxia sensitive organ. When the NMDARs are opened, they will challenge the membrane potential and cause the intracellular level of Ca^{2+} to rise. At low levels of ATP, the process of membrane repolarization is prolonged and intracellular calcium levels might raise to critical concentrations potentially leading to cell death.

Due to the key role that NMDARs play in the mammalian brain, one may expect that the structure of these receptors is different in anoxia tolerant vertebrates.

The aim of this thesis is to examine the sequence of key components of the NMDAR, with emphasis on the ubiquitous NR1 subunit in crucian carp brain, as well as participating in examining the relative expression of different NMDAR subunits in this species. Also, phylogenetic analysis will assist in the identification of the nature of the components as well as pointing out close relatives to compare function. Possibly, differences in the structure and composition of NMDARs could be involved in the anoxia survival strategy of the crucian carp.

2 Materials and Methods

2.1 Animals

The crucian carp where captured in May 2003 from Tjernsrud pond in Oslo, Norway. The fish were kept in 750-litre tanks supplied with aerated, declorinated tap water. The light conditions where 12 h light / 12 h darkness. The fish were fed daily with commercial carp food.

Crucian carp were killed by a sharp blow to the head, followed by cutting the spinal cord. The brain was rapidly sampled and snap-frozen in liquid nitrogen. It was stored at -80 °C until used.

2.2 Isolation of mRNA

Brain tissue was homogenized on ice in a glass homogenizer (Duall by Kontes) using Genoprep Direct mRNA kit. The concentration of the mRNA was assessed by measuring optical density (OD) of 1/10 dilutions of mRNA at 260 nm, using GeneQuant spectrophotometer (Amersham Pharmacia Biotech). RNA integrity was assessed by analyzing three µl (~600 ng) of mRNA on a 1 % agarose denaturing gel. Well-defined 28S and 18S rRNA bands indicated non-degraded RNA. All procedures were carried out according to manufacturer's protocol.

2.3 Primer Design to Obtain Gene Specific Clones

At the start of the project cDNA for most of the subunits of the NMDAR had not been cloned in any fish species (except for NR1 and NR2B). Thus, it was necessary to design primers based on cDNA from more distantly related vertebrates, as well as from sequences from genomic fish databases, to obtain full-length sequences of ccNR1, and expressed sequence tags (ESTs) of ccNR2A-D and ccNR3A. cDNA sequences were obtained from the NCBI web resource (http://www.ncbi.nlm.nih.gov/), while the genomic fish databases used were the FUGU BLAST server (http://fugu.biology.qmul.ac.uk/blast/) for *Takifugu* and the Ensemble server (http://www.ensembl.org/Danio_rerio/blastview) for zebrafish (*Danio rerio*). In these genomic databases sequences for fish genes were

located by blasting analogous rat sequences. Secondary to these BLAST searches, tentative gene sequences were retrieved from the genomic sequences using GENSCAN (http://genes.mit.edu/GENSCAN.html).
Available cDNA vertebrate sequences and fish sequences were aligned using ClustalX (Thompson et al., 1997) (ftp://ftp-igbmc.u-strasbg.fr/pub/ClustalX/) and analyzed using GeneDoc (Nicholas and Nicholas, 1997) (http://www.nrbsc.org/gfx/genedoc/index.html). All sequences are listed in Appendix II.

To be able to specifically clone the different subunits of the NMDAR, particular care had to be put in to alignment analyses and subsequent primer design. The degree of sequence conservation between the different NMDAR genes is high, particularly in the TM region and in between NR2 subunits (see Figure 2). To be able to clone each of the different subunits it was therefore necessary to use primers that matched areas outside TM domains. More specifically, primer syntheses were aimed at 5' ends of the genes. These regions were less conserved and allowed us to 1) construct primers that could specifically distinguish the different subunits, and 2) obtain sequences that were well-suited for phylogenetic analyses. The primers were designed to anneal to areas without known alternative splice cassettes. Further, primers were aimed at areas of the 5' ends of each gene that displayed the highest degree of sequence conservation across different species. Additionally, primers were aimed at areas that were different in between different NMDAR subunits (to avoid cloning the "wrong" subunit). Primers were made using the Primer3 software (http://frodo.wi.mit.edu/cgi-bin/primer3/primer3_www.cgi) and were ordered from Invitrogen. Primers used to clone NMDARs in crucian carp are summarized in Table 1.

Table 1. GeneRacer™ PCR Primers for Gene Specific Clones

Gene [a]	Forward primer 5'→ 3' (bp Ref. to GenBank Accession Number, CDS Segment)	Reverse primer 5'→ 3' (bp ref. to GenBank Accession Number, CDS Segment)	GenBank Accession Number [b]
ccNR1	GTTCACCTGGTGGCTGATG (1474-1492)	GGTCCAGCACCAGGAAGG (2023-2006)	Al, AF060557
ccNR2A	AGTACGACTGGCACATCTTCTC (491-512)	AATATCAATGCAGAACCCCTTG (1389-1368)	Mm, NM_008170
ccNR2B	AGCTGAAGAAGCTGCAGAGC (656-675)	TTGCTGCGAGACACCATAAC (1631-1612)	Mm, NM_008171
ccNR2C	GTACAACTGGGGCAACTTTGTG (477-498)	TGGCAGGATCAACACTCTCTAC (1267-1246)	Mm, D10694
ccNR2D	GAGGTGCTGGAGGAGTACGA (520-539)	CATAACGCTGATGCCTGTCT (1652-1633)	Mm, NM_008172
ccNR3A	AAGACATGAACTTTGAGTTTGACC (1766-1789)	TCTTCCATTCGTAGAGAGTGAGG (2095-2073)	Hs, AF416558

[a] cc = *Carassius carassius*

[b] Al = *Apteronotus leptorhynchus*, Mm = *Mus musculus*, Hs = *Homo sapiens*

Throughout this thesis, the NMDAR subunit genes for the crucian carp will be referred to as ccNR1, ccNR2A, ccNR2B, ccNR2C, ccNR2D and ccNR3A.

2.4 Full-length Cloning by RACE

2.4.1 cDNA Library

RACE (Rapid Amplification of cDNA Ends) was utilized to obtain the full-length sequence of ccNR1. RACE cDNA was made from ~1000 ng mRNA from crucian carp brain tissue using GeneRacer™ (Invitrogen). All procedures were carried out according to manufacturer's protocol.

2.4.2 GeneRacer™ Primer Design

GeneRacer™ is based on the use of GeneRacer™ specific primers that anneal to the ends of the RACE cDNA, as well as gene specific primers (GSPs). The GSPs were designed using the Primer3 resource and according to the GeneRacer™ protocol. All primers were set to have melting temperatures around 70 °C, and they were set to have a GC-clamp. The 5' GSP was constructed together with the GeneRacer™ 5' Primer as forward primer, and the 3' GSP was made with the GeneRacer™ 3' Primer as reverse primer. Synthesis of the nested gene specific primers (GSPN) followed the same procedure. See Table 2 for all ccNR1 GeneRacer™ GSPs and GSPNs. Primers were synthesized by Invitrogen.

Table 2. PCR GeneRacer™ Gene Specific Primers (GSPs) for the ccNR1 Subunit

Primer Name [a]	**Melting temp. in °C**	**Sequence 5' → 3'**	**Bp ref. to Knifefish NR1, GenBank AF060557 (CDS part)**
ccNR1 GSP 5'R1	72.2	ATAGCAAAGCCAGCCCACACCATTCC	1970-1945
ccNR1 GSP 3'F1	72.6	AGCTCCTGGGTGGCCTTGCTGATATG	1559-1584
ccNR1 GSPN 3'F2	70.1	CGTTGCACCCTTGACAATCAACAATG	1587-1612

[a] R=Reverse; F=Forward, cc = *Carassius carassius*

2.4.3 PCR Reaction Conditions for the GeneRacer™ Procedure

PCR was performed on a Mastercycler gradient (Eppendorf) using 1 µl 1/5 and 1/50 dilutions of cDNA from crucian carp brain tissue. Amplified products were analyzed on a 1 % agarose gel containing ethidium bromide (EtBr). All procedures were carried out according to manufacturer's protocol.

The 5' and 3' ends of the ccNR1 gene are rather long. According to the length of the knifefish NR1 mRNA and the corresponding placement of the primers, the 5' end would be close to 2000 bp and the 3' end would be about 2500 bp. This makes PCR amplification difficult, and calls for testing of different variants of reaction parameters such as *Taq* polymerases, PCR programs and primers. Firstly, two different *Taq* polymerases were used in this thesis, Platinum® *Taq* DNA Polymerase High Fidelity (Invitrogen) and Advantage 2 Polymerase mix with the BD TITANIUM™ *Taq* polymerase (BD Sciences Clonetech). Secondly, PCR programs were based on recommendations given in the GeneRacer™ protocol, and the length of the elongation step (polymerase action) was calculated individually for each gene. These calculations were based on sequence alignments (as previously described), where 1 kb template was estimated to require 1 minute of polymerase action. Thirdly, four sets of primers were synthesized and tested for each of the cDNA ends of ccNR1. Primers that provided positive results and were used for cloning are summarized in Table 1.

RACE cloning of the 5' end of ccNR1 was achieved using Platinum *Taq* DNA Polymerase High Fidelity. The following PCR program was used: 1) 2 min at 94 °C, 2) 30 sec at 94 °C, 3) 3 min at 72 °C 4) repeat 2-3 5x, 5) 30 sec at 94 °C, 6) 3 min at 70 °C,

7) repeat 5-6 5x, 8) 30 sec at 94 °C, 9) 30 sec at 65 °C, 10) 3 min at 72 °C, 11) repeat 8-10 25x, 12) 10 min at 72 °C, 13) hold at 4 °C.

Cloning of the 3' end of ccNR1 was achieved using Advantage 2 Polymerase mix. According to the supplier, this polymerase mix is particularly efficient in amplifying long and troublesome cDNA fragments, and should give amplification of fragments as large as 20 kb. The following PCR program was used for the initial PCR reaction (non-nested): 1) 1 min at 95 °C, 2) 30 sec at 95 °C, 3) 8 min at 72 °C 4) repeat 2-3 5x, 5) 30 sec at 95 °C, 6) 8 min at 70 °C, 7) repeat 5-6 5x, 8) 30 sec at 95 °C, 9) 8 min at 68 °C, 10) repeat 8-9 25x, 11) 10 min at 72 °C, 13) hold at 4 °C. Additionally, nested PCR was necessary to achieve amplification of the 3' end of ccNR1. This was done using 1 µl 1/100 dilutions of the initial PCR reaction, and using the following PCR program: 1) 1 min at 95 °C, 2) 30 sec at 95 °C, 3) 30 sec at 72 °C, 4) 3.5 min at 72 °C, 5) repeat 2-4 5x, 6) 30 sec at 95 °C, 7) 30 sec at 70 °C, 8) 3.5 min at 72 °C, 9) repeat 6-8 5x, 10) 30 sec at 95 °C, 11) 30 sec at 68 °C, 12) 3.5 min at 72 °C, 13) repeat 10-12 25x, 14) 10 min at 72 °C 15) hold at 4 °C.

2.5 Cloning

PCR reactions that only contained PCR products of expected sizes were ligated directly into p-GEM®-T-Easy Vector (Promega). In PCR reactions that contained bands of unexpected size, the desired bands were purified from their respective gels using Wizard® SV Gel and PCR Clean-Up Systems (Promega). These PCR fragments were then ligated into p-GEM®-T-Easy Vector (Promega). Subsequent to ligation, vectors were transformed into electro competent bacteria (*Escherichia coli*) (Invitrogen) using a specialized electroporation cuvette placed in a Gene Pulser™ electroporation machine (BioRad). The Gene Pulser™ was set to 25 µF capacitance, 1.3 kV and a 200 Ω resistance. To identify bacteria containing plasmids with insert, the bacteria were grown on agar plates containing 0.1 mg/ml ampicillin (Sigma), 100 µl IPTG (100 mM) and 20 µl X-gal (50 ng/µl) (Promega). This gives positive selection for ampicillin-resistance and negative selection against β-galactosidase activity. White colonies were thus expected to contain plasmids with inserts, and the sizes of these inserts were assessed using Platinum *Taq* PCR (with plasmid specific primers; T7 and SP6). After investigating these PCR

reactions on a 1 % agarose gel, colonies with correct inserts were incubated in LB medium containing 0.1 mg/ml ampicillin over night. Plasmid DNA from 10 positive colonies were then extracted using Wizard® *Plus*SV Minipreps DNA purification system (Promega). Plasmid DNA yields were determined by OD260 measurements, and 450 ng of plasmid DNA was sent for sequencing (using M13F+R primers).

2.6 Sequencing

Plasmids were sequenced at the MegaBACE lab, Department of Biology and Molecular Biosciences, Centre for Ecological and Evolutionary Synthesis (CEES), University of Oslo, Norway. During the sequencing part of this thesis, the MegaBACE lab was experiencing problems with the stability of the sequencing facility. Consequencely, only short sequences (300-600 bp) were obtained. To be able to cover the rather large ccNR1 mRNA, this resulted in two extra rounds of sequencing of both the 5' and the 3' end clones. Primers used for these reactions were designed using Primer3 and synthesized by Invitrogen. They are summarized in Table 3. These primers had melting temperatures ~50 °C to match the sequencing reaction conditions at the MegaBACE facility.

Table 3. Extra Sequencing Primers for the ccNR1 Subunit

Primer name [a]	**Melt. temp. in °C**	**Sequence 5' → 3'**	**Bp ref. to knifefish NR1, GenBank AF060557 (CDS part)**
ccNR1 5'F1 [b]	51.2	GAACCAAGTGTACGGAAG	138-155
ccNR1 5'R6 [d]	50.4	CTGTAATGAGCATATTTTCTG	1106-1086
ccNR1 5'F2 [d]	54.7	TCTCTGCCAGTGAGGAAG	713-730
ccNR1 5'R5 [b]	49.6	TAGTTAGTCCCTGGTATTTG	1666-1647
ccNR1 3'F5 [c]	52.0	CACGTAGTTTTTCAGCAAG	1919-1937
ccNR1 3'F6 [e]	50.4	CTCACCTTTGAGAATATGG	2470-2488
ccNR1 3'R2 [e]	51.4	CACACTTATAGGGGATTTTC	3882-3863 rel. to cc 'ATG'
ccNR1 3'R1 [c]	50.6	CATCTTAGTCATCTGCAATC	4354-4335 rel. to cc 'ATG'

[a] The 'F' and 'R' in the primer names means 'Forward' and 'Reverse', respectively. cc= Carassius carassius
[b] These primers were involved in the second round of sequencing (nested sequencing) on the cloned 5' cDNA template.
[c] These primers were involved in the second round of sequencing (nested sequencing) on the cloned 3' cDNA template.
[d] These primers were involved in the third round of sequencing (nested nested sequencing) on the cloned 5' cDNA template.
[e] These primers were involved in the third round of sequencing (nested nested sequencing) on the cloned 3' cDNA template.

2.7 Aligning Sequences

After sequencing by MegaBACE, the raw sequences were examined to assess their quality. This was performed in BioEdit (Hall, 1999). After removing the clearly biased sequences, multiple alignments were performed using ClustalX. Consensus sequences were made using GeneDoc.

2.8 Protein Sequence and Structure Features

The full length NR1 amino acid sequence was deduced by translating the ccNR1 mRNA using GeneDoc software. To be able to assess protein properties, the ccNR1 protein sequence was aligned with rat, knifefish and zebrafish NR1 using ClustalX and GeneDoc. The TM topology was also supported by analyzing the ccNR1 through the web server TMHMM Server v2.0 (http://www.cbs.dtu.dk/services/TMHMM-2.0/). The signal peptide sequence (SS) was identified using the freely available SignalP 3.0 web server (http://www.cbs.dtu.dk/services/SignalP/), and N-glycosylation and phosphorylation sites were predicted using the Prosite server (release 20.13) (http://expasy.org/prosite/), the NetPhos 2.0 server (http://www.cbs.dtu.dk/services/NetPhos/) and the NetPhosK 1.0 Server (http://www.cbs.dtu.dk/services/NetPhosK/). A 3D structure of the ccNR1 ligand binding domain was generated using DeepView (http://au.expasy.org/spdbv/), which in turn used the crystal structure of rat NR1 (Protein Data Bank ID 1PB7) as template.

2.9 Phylogenetic Analysis

440-600 bp regions of crucian carp NMDAR mRNA were aligned with sequences from other vertebrates using ClustalX. The accession numbers for NMDAR genes used are summarized in Appendix II. BLAST searches in available zebrafish databases (see section 2.3) identified two paralogs of NR1, as well as two paralogs of all NR2 subunits. These were included in the phylogenetic analyses. GeneDoc were used to create files compatible with phylogenetic analyses calculated and bootstrapped using the neighbor-joining method through the non-profit software Phylip (http://bioweb.pasteur.fr/seqanal/phylogeny/phylip-uk.html). Unrooted phylogenetic

diagrams were made using freely available software Treeview (http://taxonomy.zoology.gla.ac.uk/rod/treeview.html)

2.10 Primer Design for Real-Time RT PCR

For future gene expression analyses of crucian carp NMDAR subunits, sets of real-time RT PCR primers were made, see Table 4. These primers were made using the LightCycler Probe Design Software (version 1.0, Roche), and designed to specifically amplify each of the different subunits. Amplicon sizes were set to 200-300 bp. The primers were synthesized by Invitrogen.

Table 4. LightCycler Primers for Real-Time RT PCR

Gene [a]	**Forward primer 5'→ 3' (bp Ref. to GenBank Accession Number, CDS Segment)**	**Reverse primer 5'→ 3' (bp ref. to GenBank Accession Number, CDS Segment)**	**Product size**	**GenBank Accession Number** [b]
ccNR1	TATGATCGTTGCACCCT (1581-1597)	GTAAAGCATCACCGCC (1782-1767)	202 bp	Al, AF060557
ccNR2A	AAGGTCGGATACCTGA (929-944)	ATGTCCCCAAATGAGTT (1196-1180)	268 bp	Mm, NM_008170
ccNR2B	AAGGCTTCTGTATCGAC (1373-1389)	CTATGAAGGGCACGGA (1591-1576)	219 bp	Mm, NM_008171
ccNR2C	GGATTCATTCCCGATGG (922-947)	ATACAGGGTATCGCATCT (1159-1142)	238 bp	Mm, D10694
ccNR2D	CGTTCAATAATGAGGGC (1091-1107)	CACGGAGTCCCTAATG (1346-1331)	256 bp	Mm, NM_008172
ccNR3A	ACGGGAAATATGGAGC (1805-1820)	CATGGACCAGTGCAAC (2031-2016)	227 bp	Hs, AF416558

[a] cc = *Carassius carassius*

[b] Al = *Apteronotus leptorhynchus*, Mm = *Mus musculus*, Hs = *Homo sapiens*

3 Results

3.1 NMDAR Subunit Sequences

The full-length mRNA sequence of ccNR1 and ESTs of ccNR2A-D and ccNR3A were found, as described in Materials and Methods (see Appendix IV for sequences).

Two paralogs were found for ccNR1, ccNR2A and ccNR2D subunits. Because of the close relationship with the zebrafish NMDAR subunits, the sub-naming of the crucian carp subunits and paralogs were determined based on the closest zebrafish paralog according to the phylogenetic analysis in Figure 6 and 7, e.g., for the ccNR1 subunit, the phylogenetically closest zebrafish paralog would be the drNR1.1 and the subsequent naming for the crucian carp subunit would be ccNR1.1. For cucian carp NMDAR paralogs, an extra sub-level of naming was applied and the zebrafish relative naming resulted in the names: ccNR1.1.1, ccNR1.1.2, ccNR2A.1.1, ccNR2A.1.2, ccNR2B.1, ccNR2C.1, ccNR2D.1.1 and ccNR2D.1.2. When comparing the sequences of both paralogs of a crucian carp NMDAR subunit with another subunit, there will be made an average and the naming will step up one level, e.g., comparing other sequences with the sequences for the ccNR2D.1.1 and ccNR2D.1.2 paralogs, they will collectively be referred to as ccNR2D.1.

Nucleotide sequences of the two ccNR1.1 paralogs diverged by 3.3 %, with 48 out of 1453 nucleotides being different. This area stretched from amino acid 61 to 545. Of the 48 nucleotide mutations, only two resulted in changes of the amino acid composition. The first, threonine (T) → serine (S) was seen in position 96, and the second, methionine (M) → threonine (T), was seen in position 433. The N1 and C2' cassettes were found in both ccNR1.1 paralogs (see Figure 5 in section 3.2 for positions in the protein). Whereas, a novel splice cassette, consisting of the amino acids 'NTSG', was found in the ccNR1.1.1 paralog (Figure 5, box at position 464-467). Nucleotide sequences of the two ccNR2A.1 paralogs diverged by 6.6 %, with 37 out of 559 nucleotides being different. This brought along 14 differences in between amino acid sequences and the area aligns with amino

acid 238-424 in ccNR1.1.1. Finally, the two paralogs of ccNR2D.1 also diverged by 6.6 %, with 47 out of 1094 nucleotides being different. This brought along 9 differences in between amino acid sequences and compares to the amino acid area 172-536 in ccNR1.1.1.

It was not possible to use the nucleotide sequence to determine which type of NR3 subunit that had been cloned, as the sequence is located in a highly conserved area of NR3A and NR3B. However, using the amino acid sequence provided evidence for it being NR3A (see details in section 3.3).

Ranging from amino acid 244 to 426, ccNR1.1 displayed 33-39 % nucleotide homology to the different ccNR2 subunits, and ranging from amino acids 497 to 595, ccNR1.1 displayed 32 % nucleotide homology to the ccNR3A subunit. In between ccNR2 subunits the homology was 44-58 % measuring in the amino acid region 244 to 426 in ccNR1.1.1. Further, in the same area (ccNR1.1.1 amino acid 244 to 426) the ccNR1.1 subunit showed 72-84 % homology to other vertebrate NR1 subunits (these vertebrates can be found in Figure 7). Finally, the sequences defining the ccNR2 phylogenetic analysis (matching area ccNR1.1.1 amino acid 244 to 469), ccNR2A.1, ccNR2B.1, ccNR2C.1 and ccNR2D.1 showed 60-90 %, 56-78 %, 59-90 % and 50-90 % homology to their respective vertebrate NR2 subunits (these vertebrates can be found in the phylogenetic tree for the NR2 subunits in Figure 8).

3.2 Crucian Carp NR1 Structure and Special Features

The deduced ccNR1.1 subunit protein sequence can be found in Appendix IV and is represented by the most abundantly expressed paralog, ccNR1.1.1, as determined by the existence in 8 out of 12 clones. Figure 5 shows an alignment of ccNR1.1.1 with rat, zebrafish and knifefish NR1. It displays a high degree of conservation in the TM domains, TM1-TM4, the pore-forming element, P, and the glycine binding areas S1 and S2 (black bars). The black arrow points to known ligand binding residues (for review on the NR1 structural domains, see Chen and Wyllie 2006). The high degree of similarity in TM domains between ccNR1.1.1 and knifefish NR1 suggests similar NR1 topologies in

these two species. This was supported by the TMHMM Server (v2.0) (prediction of TM helices in proteins). The TM helices were predicted to span the amino acids 581-600, 655-677 and 835-857 starting outside the cell and ending inside. The putative channel gating segment 'SYTANLAAF' at the N-terminal of TM3 was found to be highly conserved between fish and mammals. Four phosphorylation sites were suggested by the phosphorylation prediction servers NetPhos 2.0, NetPhosK 1.0 and Prosite and 10 positions for N-glycosylation were found with the Prosite scan server. All sequences used in the alignment contained the N1, C0 and C2' splice cassettes, whereas only zebrafish and knifefish contained the C1 and C1' cassettes, and knifefish alone contained the C1'' cassette. One N-glycosylation site, 'NTSG' at ccNR1.1.1 amino acid 464-467, was not found in other available vertebrate sequences.

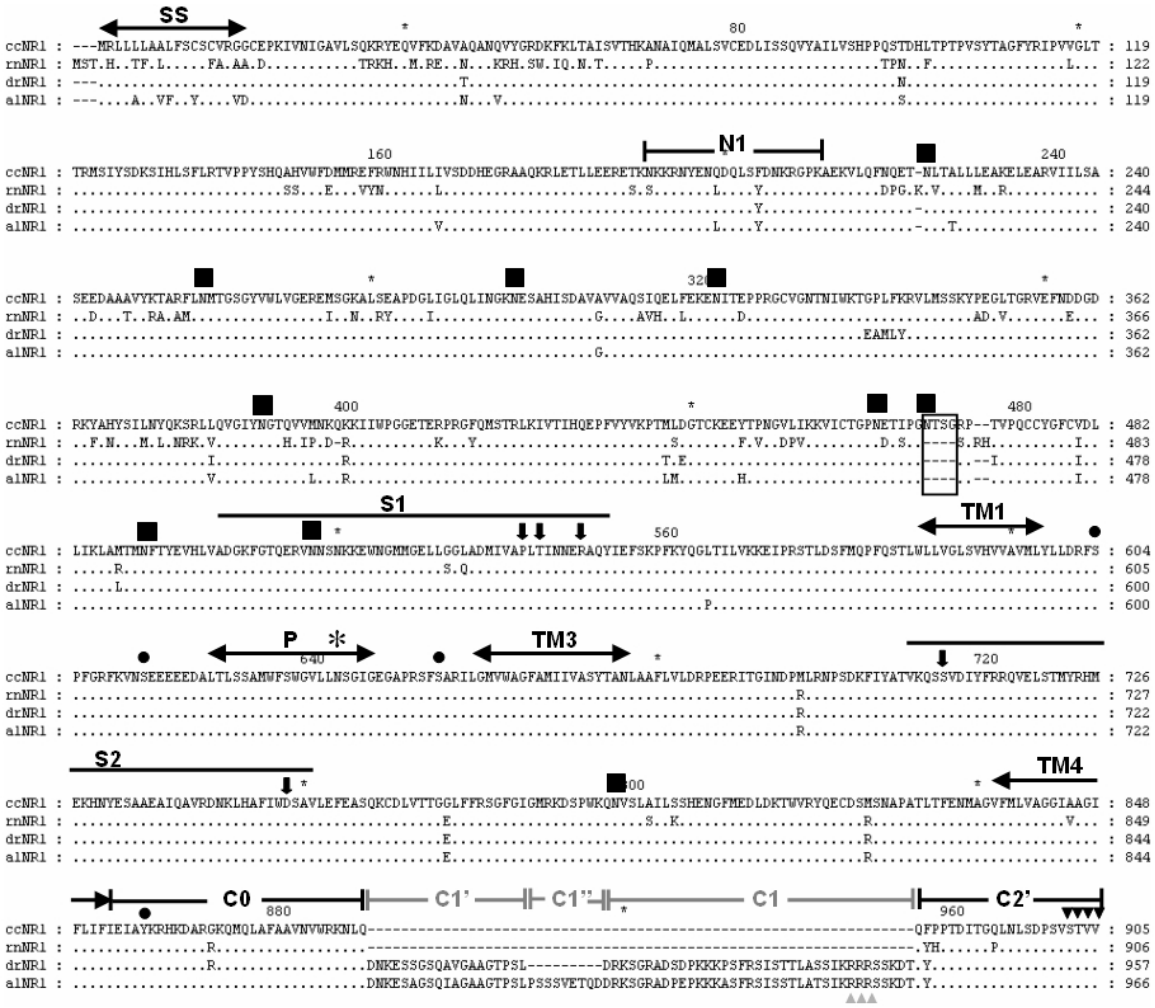

Figure 5. Amino acid comparisons of crucian carp (cc) ccNR1.1.1 with rat (rn) NR1, zebrafish (dr) NR1 and knifefish (al) NR1. Residues identical to ccNR1.1 are indicated by a *dot* (.) and deletions/gaps are indicated by a *hyphen* (-). Amino acid positions are found to the right and above the alignment, and sequence names are found to the left. The signal sequence (*SS*) is found at the start of the ccNR1.1 sequence, and *TM1*, *TM2* and *TM4* indicate the putative transmembrane segments. *P* represents the proposed ion pore, while S1 and S2 represent glycine ligand binding segments. Known glycine ligand binding residues are indicated by *black arrows*. N-glycosylation sites and phosphorylation sites are pointed out by *black squares* and *black circles*, respectively. An *asterisk* (*) is found above the Mg^{2+} binding asparagine residue in the pore element. *N1*, *C1*, *C1'*, *C1''* and *C2'* splice cassettes are indicated. The 'NTSG' cassette found in crucian carp is represented by a *box* (residues 464-467). Areas with *black triangles* are recognized by the PSD95 protein, and the area with *grey triangles* indicates an ER retention signal.

The crystal structure of the rat NR1 ligand binding domain (Protein Data Bank ID 1PB7) was utilized to determine the 3D (tertiary) structure of corresponding regions of crucian carp ccNR1.1.1 and zebrafish NR1 paralogs (Figure 6). All amino acids that were found to be different between crucian carp and zebrafish were located outside the glycine-binding structure. The 'NTSG' cassette was contained in an unresolved part of the rat NR1 crystal structure.

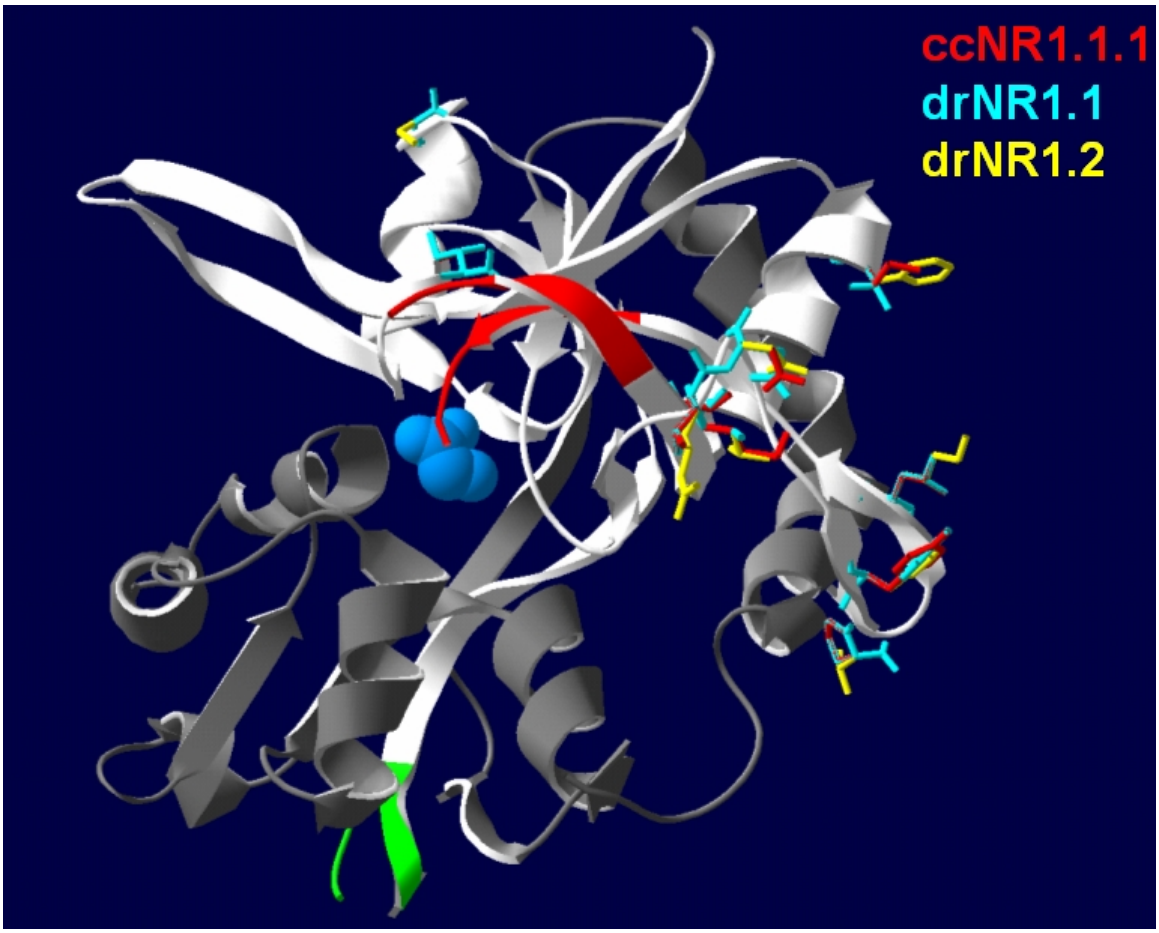

Figure 6. 3D (tertiary) structure of N-terminal glycine binding extracellular domain of the ccNR1.1.1 subunit. The rat NR1 crystal structure (Protein Data Bank ID 1PB7) was used as template. In the white region, that spans the S1 segment in Figure 5, the mutations were assessed in two zebrafish NR1 paralogs and the crucian carp ccNR1.1.1 paralog. All differences in this part of the protein were located on the surface of the structure and are presumably not affecting the binding of glycine (fragment in blue). Green β-sheet/coil indicate sequences entering and leaving transmembrane regions. Red β-sheet/coil indicate sequences entering and leaving the splice cassette, 'NTSG', reported in crucian carp. Aligning, imaging and colouring were made with the DeepView software. cc = *Carassius carassius*, dr = *Danio rerio*

3.3 Phylogenetics Analysis

ESTs for all NMDAR subunits were obtained from *Trachemys scripta*, using primers meant for cloning of the same genes in crucian carp. This was performed by others at our research group. These sequences were included in phylogentic analyses whenever they overlapped with crucian carp sequences.

Figure 7 shows an unrooted phylogenetic tree, placing the two ccNR1.1 paralogs, ccNR1.1.1 and ccNR1.1.2, in an evolutionary context together with the zebrafish drNR1.1 and other teleosts. This tree was made by aligning sequences as defined by nucleotides 1025-1623 of knifefish NR1. This was the only region containing both of the ccNR1.1 paralogs overlapping with the two paralogs in zebrafish. The colouring of Figure 7 corresponds with the colouring of Figure 6.

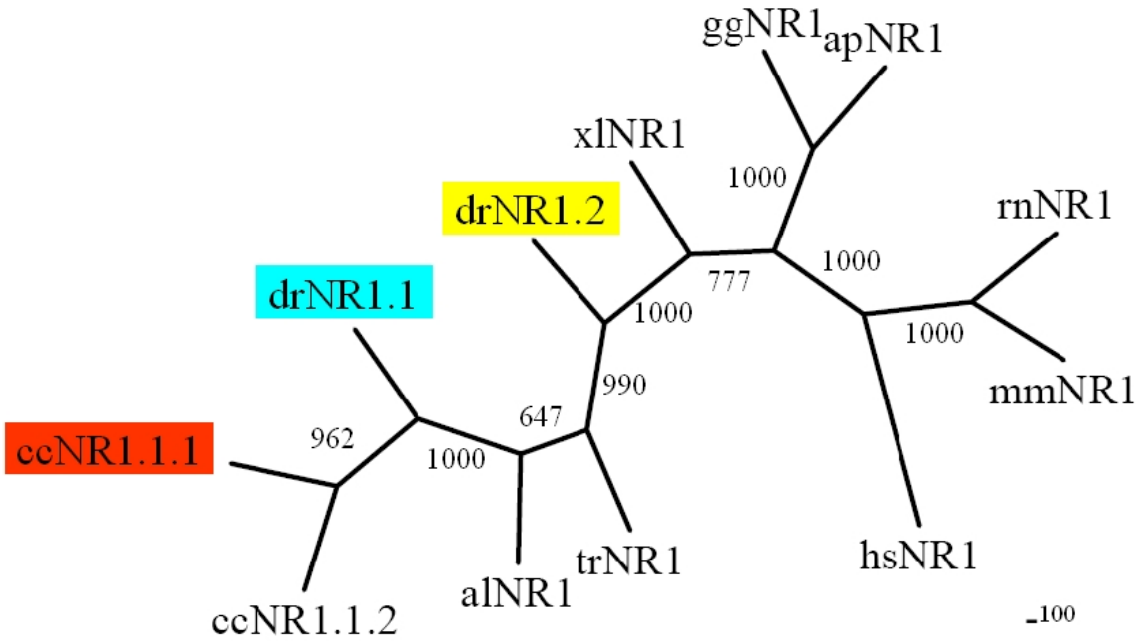

Figure 7. Phylogenetic tree for NMDAR subunit NR1. Species included are al = *Apteronotus leptorhynchus*, ap = *Anas platyrhynchus*, cc = *Carassius carassius*, dr = *Danio rerio*, gg = Gallus gallus, hs = *Homo sapiens*, mm = *Mus musculus*, rn = *Rattus norvegicus*, tr = *Takifugu rubripes*, xl = *Xenopus laevis*. The sub-numbering of the subunits for cc and dr is referring to paralogs found in the organism. The colours correspond to the colouring of Figure 6. The tree is based on the alignment of the alNR1 mRNA CDS area 1025-1623 (GenBank AF060557), which was generated using ClustalX. The phylogenetic relations were calculated and bootstrapped using the neighbor-joining method. The numbers at branch points are the bootstrap values from 1000 iterations.

Figure 8 shows an unrooted phylogenetic tree, placing the ccNR2A.1-D.1 subunits in an evolutionary context. The identity of the different ccNR2 subunits was confirmed as they were positioned among equal subunits in the tree. This tree was made by aligning sequences as defined by nucleotides 850-1403 of knifefish NR2B. This was the only gene region containing sequences for all ccNR2 subunits.

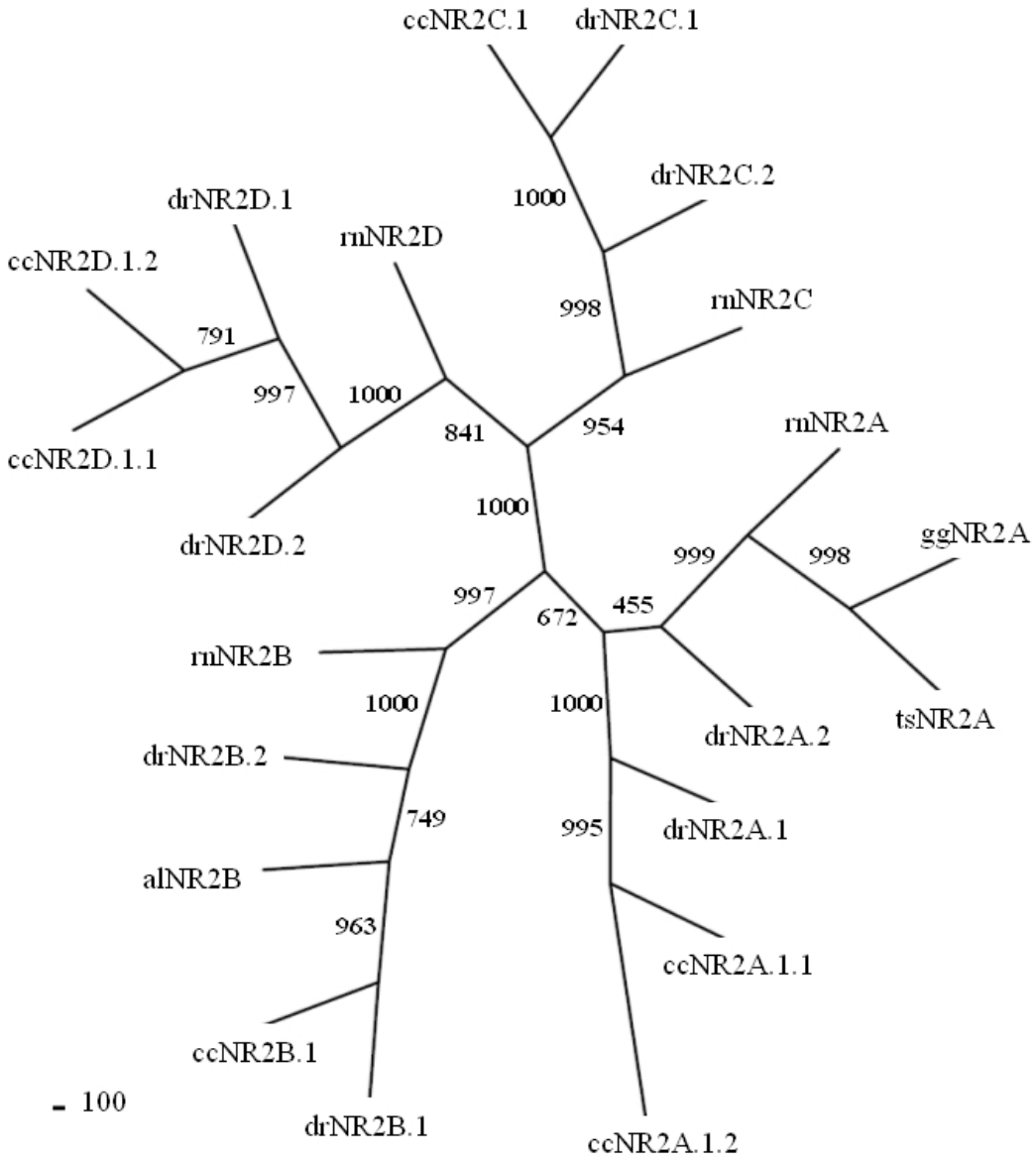

Figure 8. Phylogenetic tree for NMDAR subunits NR2A-D. Species included are al = *Apteronotus leptorhynchus*, cc = *Carassius carassius*, dr = *Danio rerio*, gg = *Gallus gallus*, rn = *Rattus norvegicus*, ts = *Trachemys scripta*. The sub-numbering of cc and dr subunits refers to different paralogs. The tree is based on an alignment defined by nucleotides 850-1403 of knifefish NR2B, and was generated using ClustalX. The phylogenetic relations were calculated and bootstrapped using the neighbor-joining method. The numbers at branch points are the bootstrap values from 1000 iterations.

The NMDAR subunits NR3A and NR3B were only available for human, mouse and rat at the time of primer synthesis and phylogenetic analyses in this thesis. Therefore, no phylogenetic tree for the NR3 family is shown. However, alignments were made defined by nucleotides 1790-2072 of rat NR3A (GenBank AF073379). These alignments revealed that the obtained ccNR3A EST (283 nucleotides) displayed varying similarity to vertebrate NR3A and NR3B, e.g. 73 % homology to rat NR3A and 75 % homology to rat NR3B was found. Based on these nucleotide comparisons it was not possible to define ccNR3 to be NR3A or NR3B. The area was equally conserved between the two. Therefore, to confirm that the ccNR3A subunit had been cloned, a BLAST search was executed on deduced amino acid sequence. The 93 resulting amino acids showed 86-100 % similarity to vertebrate NR3A, while it showed 77-81 % similarity to the vertebrate NR3B. More specifically, the 93 deduced ccNR3A amino acids were 87 % homologous to rat NR3A and 81 % homologous to rat NR3B.

Finally, Figure 9 shows an unrooted phylogenetic tree to place the crucian carp ccNR1.1 and ccNR2 subunits in an evolutionary relationship to each other. The crucian carp paralogs available were grouped together and the ccNR2 subunits sharing features (NR2A/NR2B and NR2C/NR2D, review by Dingledine et al., 1999) also displayed proximity.

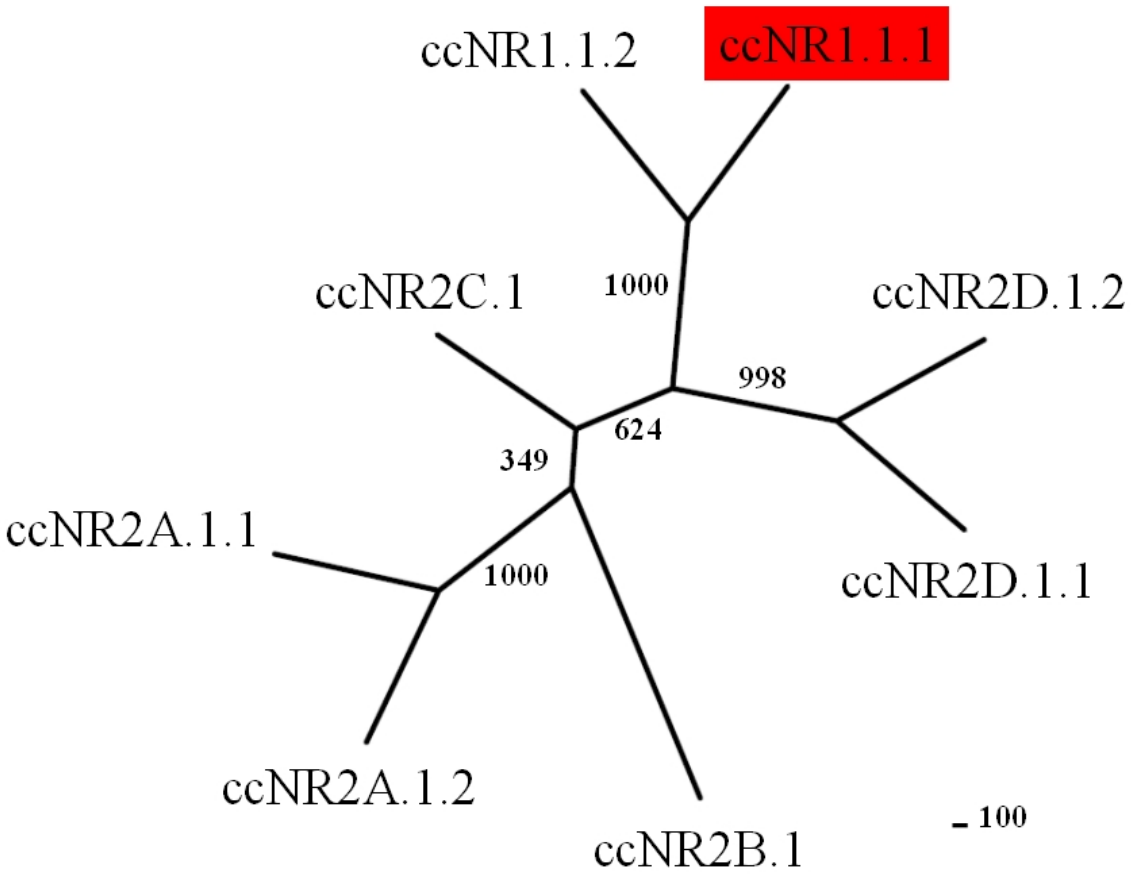

Figure 9. Phylogenetic tree for crucian carp NMDAR subunit ccNR1.1 and ccNR2A.1-D.1. cc = *Carassius carassius*. The sub-numbering of the ccNR1.1, ccNR2A.1 and ccNR2D.1 subunits is referring to paralogs found in the organism. In addition, all subunits are numbered to reflect the evolutionary closest zebrafish paralog, see Figure 7 and 8. The colour corresponds to the colouring of Figure 6 and 7. The tree is based on the nucleotide alignment of the subunits in the area of the ccNR1.1.1 protein amino acid 244 to 426. It was generated using the output of a ClustalX multiple alignment and was calculated and bootstrapped using the neighbor-joining method. The numbers at branch points are the bootstrap values from 1000 iterations.

4 Discussion

This thesis reports the cloning and sequencing of the full-length NMDAR subunit ccNR1.1 mRNA and of ESTs of the subunits ccNR2A.1-D.1 and ccNR3A. The ccNR1.1 sequence and its features have been assessed and phylogenetic trees for all subunits have been computed. This was done to confirm their identity and to place them in an evolutionary context. Further, sets of real-time RT PCR primers were made for all subunits. These primers will enable future analyses of mRNA expression in normoxic and anoxic crucian carp.

4.1 PCR Optimization

RACE PCR on the ccNR1.1 subunit proved to be difficult, particularly in its 3' end. To obtain functional assays, it was therefore necessary to optimize different reaction parameters, like *Taq* polymerases, PCR programs and primers.

In the 3' end this implied the use of a different *Taq* polymerase, since the Platinum® *Taq* seemed to be operating close to its limits. The Advantage 2 polymerase mix was used, as this polymerase mix is supposed to be particularly useful for difficult templates. In addition to containing the modified and more robust BD TITANIUM™ *Taq* polymerase, it contains a proof reading enzyme, and is reported by the manufacturer to amplify DNA templates as large as 20 kb.

The fact that a different *Taq* polymerase had to be used to achieve successful 3' RACE of ccNR1.1 might have to do with the quality of the primers. In the GeneRacer™ protocol the linker-specific primers (GeneRacer™ 5' and 3' primers) were listed as having melting temperatures between 72 and 78 °C. When this was calculated using the Primer3 software, these primers were assigned melting temperatures ranging from 65 and 69 °C. Further, GSP RACE primers were designed using Primer3, and they were given Primer3 calculated melting temperatures ranging from 70 to 72 °C (Table 2). Thus, there was a large discrepancy in melting temperatures between GeneRacer™ primers and GSPs. This was not discovered until late in course of the project, and brought along large variations

in melting temperature (~4.4°C) within every single primer pair. The basis of touchdown PCR is to start out with annealing temperatures similar to those of primer melting temperatures, and to gradually lower it to get a more efficient amplification as PCR products are accumulating (Don et al., 1991). Primers with different melting temperatures will require different annealing temperatures, and the closer the melting temperatures of a primer pair, the larger their potential of success. Thus, the primers used for 3' RACE of ccNR1.1 were far from ideal.

4.2 NMDAR Subunit Sequences

There are greater sequence similarities in between ccNR2 subunits than between ccNR2 and ccNR1.1 (Figure 9) or ccNR3A. All ccNR2 ESTs were obtained in the 5' end (N-terminal) of the gene. This was done to be able to distinguish between them in PCR reactions and to enable phylogenetic analyses.

4.2.1 Primer Design

Primers designed for EST cloning of ccNR1.1, resulted in an amplicon containing the ligand binding loop S1, the pore element P and the transmembrane segment TM3 (Figure 2). The primers where placed in highly conserved regions. These turned out to represent β-plate and α-helix structures (data not shown). These structures are considered important for protein function and tend to be conserved across species (Sitbon and Pietrokovski, 2007). Positions for primers were Primers for EST cloning of ccNR3A were aimed toward the membrane pore element P, the transmembrane TM3 and part of the ligand binding loop S2. These ccNR3A elements are highly conserved between species, as well as between ccNR3 subunits, especially on the nucleotide level (see Figure 2 and Figure 5, section 3). Thus, the ccNR3A identity could not be verified via nucleotide BLAST, and could only be determined via amino acid BLAST. Further, the highly conserved sequence excluded accurate assessment of NR3 phylogenetics. This would have been possible, had the ccNR3A EST been retrieved from the less conserved pre-transmembrane region (as was done for ccNR2A.1-D.1).

4.2.2 Crucian Carp Paralogs

The two paralogs found for ccNR1.1, ccNR2A.1 and ccNR2D.1 displayed DNA mutation rates of 3.3 %, 8.3 % and 8.1 %, respectively. These mutations affected the amino acid sequence with a rate (functional mutation rate) of 0 %, 36 % and 14.3 %. The sequences investigated were located to analogous regions of the 5' ends (ccNR1.1.1 amino acid area 238-381, Figure 5). The DNA mutation rates tell us that the ccNR2A.1 and ccNR2B.1 genes are mutating twice as fast as the ccNR1.1 gene. Speculatively, mutations in the ccNR1 gene may produce dysfunctional proteins that are selected against. The functional mutation rates reflect this possibility, as no amino acid changes are seen in the ccNR1.1 protein. This indicates the need for uniform and stable NR1 function. In the light of the dose-model proposed by Force et al. (1999), both ccNR1 paralogs might be needed to cover the demand for NR1 subunits. Thus, both copies must retain their functionality. Further, the high amino acid mutation rates of NR2A.1 and NR2B.1 indicate that functional changes in this region of ccNR2 proteins are not detrimental for their function. Indeed, for ccNR2A every third mutation ends in changes in amino acid composition. The high amino acid mutation rate may be due to two factors. Firstly, the mutations may not affect protein function. Secondly, the mutations may occur in a part of the protein where functional changes are allowed.

In accordance with the DDC model by Force et al. (1999) the paralogs of ccNR2A.1 and ccNR2D.1 might have become subfunctionalized or neofunctionalized. The wider variety of NMDAR subunits in crucian carp could reflect a need for seasonal change in subunit composition. Indeed, in another cyprinid, the zebrafish, the expression of NMDAR subunit paralogs have been proven to vary during the course of embryonic CNS development. While the zebrafish paralog NR1.1 mRNA is found in the brain, retina and spinal cord 24 hours postfertilization (hpf), the NR1.2 is expressed only in the brain and detected 48 hpf. The NR2 paralogs displayed a much more diversified expression: both NR2A paralogs were expressed in the brain 48 hpf, no NR2B or NR2C paralog could be detected embryonically and while the NR2D.1 was expressed in the forebrain, retina and spinal cord 24 hpf, the NR2D.2 was only found in the retina (Cox et al., 2005). The regional expression of the ccNR2A.1 and ccNR2D.1 paralogs in crucian carp remains to

be assessed, along with the confirmation of the existence and expression of paralogs for ccNR2B and ccNR2C.

Another analysis performed of the two ccNR1.1 paralogs revealed 48 nucleotide mutations within the 5' region of the gene (amino acid 60-545 in Figure 5). These mutations resulted in 2 differences in amino acid composition (amino acid 96 and 433). In general, the amino acids are conserved in these two local regions of the gene (Figure 5). This implies a functionally important segment where amino acid transitions would be undesired to preserve protein function. However, interestingly, the two residues also differ between the other species compared in Figure 5. Taken together, the transitions between the two crucian carp ccNR1.1 paralogs would not likely alter the paralogs' function.

4.3 Crucian Carp NR1 Subunit Structure and Function

4.3.1 The N-terminal and C-terminal Splice Cassettes

The multiple alignment shown in Figure 5 shows the high degree of NR1 protein conservation between crucian carp, rat, zebrafish and knifefish. All four species express NR1 with the alternative splice cassette N1 and the alternative C-terminal splice cassette C2'. The ccNR1 N1 cassette shows 90-95 % similarity to the zebrafish and knifefish N1 cassette, and 86 % similarity to the rat N1 cassette. The amino acids that differ tend to retain the physical properties of the protein. Thus, the overall hydrophilic profile of N1 is preserved in crucian carp, as the positively charged residues in ccNR1 position 189,190,191,204,205 and 208 are retained. Its function as a modulator of polyamine potentiation and proton inhibition (Zheng et al., 1994) do not seem to change. Further, the N1 cassette was not present in all clones obtained from crucian carp, leaving the crucian carp with the ability of varying how NMDARs will be influenced by protons and polyamines.

The C0 cassette is found immediately after TM4 and is present in all known splice variant of the NR1 (Dingledine et al., 1999) (see Figure 5). The C0 cassette is known to host one of the two calmodulin binding sites positioned in the NR1 C-terminal. These function to

desensitize the NMDAR in the presence of Ca^{2+} (Ehlers et al., 1996). Only one amino acid differed in this cassette compared to rat and zebrafish, suggesting that the function of inhibition by calmodulin is preserved in crucian carp.

The C2 cassette of the NR1 C-terminal remains to be found in teleosts. However, the alternatively spliced C2' cassette, the C1 cassette and the teleost specific C1' and C1'' cassettes have been found to be expressed (Bottai et al., 1998; Cox et al., 2005; Tzeng et al., 2007). The C2' cassette includes a binding site for the PSD95 protein with the motif 'STVV' (see Figure 5). This has been proposed to link the NMDAR to the post-synaptic density for correct location at the synapse (Kornau et al., 1995). The motif is completely conserved between crucian carp and the other species in the alignment. Thus, ccNR1.1.1 is likely to bind PSD95. Further, this motif is needed to mask the ER retention signal 'RRR' present in the C1 cassette (Standley et al., 2000) (pointed out by the grey triangles in Figure 5). Whether or not the C1 cassette and the teleost specific cassettes C1' and C1'' are expressed in crucian carp, remains to be investigated.

4.3.2 The NTSG Cassette

Figure 5 and 6 reports a new 'NTSG' cassette in crucian carp not reported to be expressed in other species. This sequence is predicted by the Prosite scan server to function as an N-glycosylation site, together with nine other sites in the protein. These nine sites were found to be conserved between rat, zebrafish, knifefish and crucian carp, indicating important roles. N-glycosylation might serve to assist the proper folding of a protein, but it may also function as anchor points for extracellular molecules. For ionotropic glutamate receptors this type of glycosylation has been observed to influence ligand binding activity, receptor physiology, susceptibility to allosteric modulation and sometimes trafficking to and from the membrane of the receptor (Standley and Baudry, 2000). In Figure 6 the 'NTSG' cassette of crucian carp aligns with an unresolved extracellular part of the rat NR1 crystal structure. The fact that it has not been resolved indicates that it represents a 'loose' part of the structure, and indicates that it is situated on the surface of the protein. The former means that the sequence is not stable as it is, and makes it a likely candidate for interaction with other molecules. The latter makes it very

likely for the 'NTSG' to be N-glycosylated. Indeed, this cassette is inserted in a cysteine-rich NR1 region, loop 1, ascribed important roles in subunit assembly and in the allosteric coupling of NR1 glycine binding and NR2 glutamate binding (Furukawa and Gouaux, 2003).

After using the nucleotide version of the 'NTSG' region to search genomic sequence databases, analogs were found in zebrafish and *Takifugu*. While, 100 % conservation was found between crucian carp and zebrafish, less conservation was found between crucian carp and *Takifugu*. In *Takifugu* the sequence does not make up an N-glycosylation site. Further, the sequences surrounding the NTSG site were well conserved across crucian carp, zebrafish and *Takifugu*, especially on the level of amino acid (Figure 10). The 'NTSG' cassette could not be found in other organisms. Thus, the 'NTSG' cassette seems to be teleost specific and it is very well conserved between crucian carp and zebrafish. Like crucian carp, the zebrafish, and many cyprinids, has been found to cope with relatively severe hypoxic conditions (Rees et al., 2001; Roesner et al., 2006), and this N-glycosylation site could speculatively play a neuroprotective role in the adaptation of the NMDAR to life with little or no oxygen.

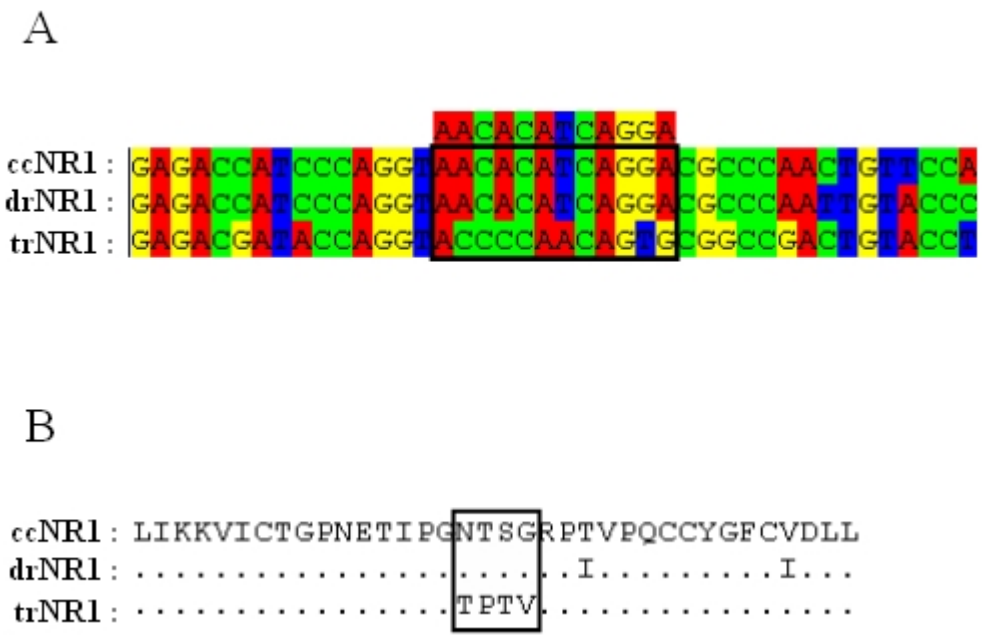

Figure 10. Multiple alignments of teleost NMDAR subunit NR1 'NTSG' site related to the box in Figure 5. Sequence names are found to the left. cc = *Carassius carassius*, dr = *Danio rerio*, tr = *Takifugu rubripes*. Sequences for zebrafish and *Takifugu* were found in public sequence databases. The alignments were prepared using ClustalX. Colouring and translation to amino acids were generated using GeneDoc. (A) Multiple alignment of nucleotides spanning the 'NTSG' site (*box*) for crucian carp, zebrafish and *Takifugu*. (B) Multiple alignment of the deduced amino acids spanning the 'NTSG' site (*box*) for crucian carp, zebrafish and *Takifugu*. Residues identical to the crucian carp sequence are denoted as *dots* '.'.

All amino acid differences occurring in ccNR1.1 or drNR1 sequences in Figure 6 are situated on the surface of the protein structure. They do not seem to affect the glycine ligand binding pocket.

4.4 Gene Expression in Crucian Carp NMDAR Genes

The NR2 subunit composition of NMDARs changes during development in the vertebrate brain. In rat, NR2B and NR2D are highly expressed prenatally, while NR2A and NR2C are first detected near birth (Monyer et al., 1994). Controlling this subunit switch is clearly important, as different NR2 subunits differ in their sensitivity to Mg^{2+} block, in their glycine sensitivity and in their deactivation time.

The real-time RT PCR primers (see Table 4) were used by others at our research group to measure gene expression levels of NMDAR subunits in crucian carp brain tissue. The NR2 subunit composition is of particular interest, since it is an important determinant of

receptor property. This composition is shown in Figure 11, and indicates that crucian carp brain tissue has a high expression of ccNR2B.1 and ccNR2D.1 (amounting to 48.1 % and 32.4 % of the overall NR2 expression), and a low expression of NR2A.1 and NR2C.1 (amounting to 12.5 % and 7 %). In an experiment measuring mRNA levels of NR1, NR2A, NR2B, NR2C, NR2D and NR3A in different rat brain regions, NR1 expression was found to be about 4 times higher than the combined expression of NR2A-D and NR3A (Goebel and Poosch, 1999). The NR2 data of that experiment was used to calculate relative NR2 subunit abundances in rat brain (Figure 11). Compared to their relative expression in the crucian carp brain, rat NR2 subunits seem to display a more evenly divided expression.

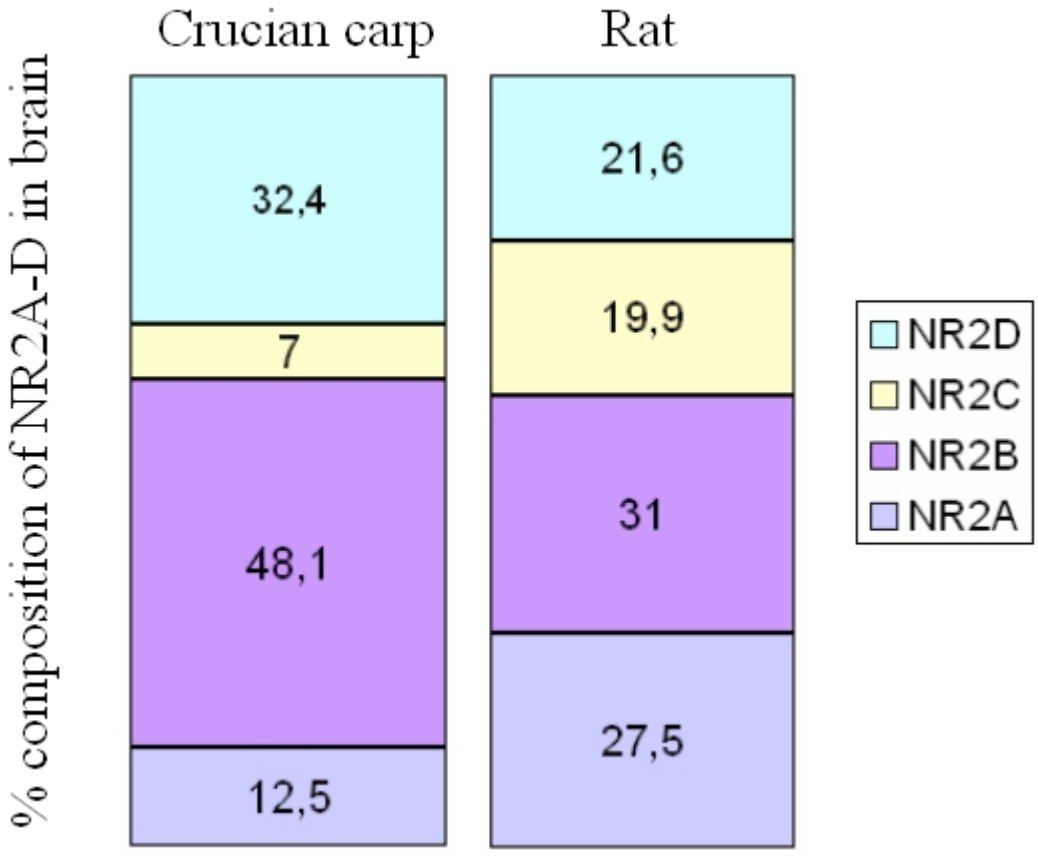

Figure 11. % composition of NMDAR subunit NR2A-D mRNAs in normoxic crucian carp and rat brain. Measurement for crucian carp was performed using real-time RT PCR with primers from Table 4, n=6. Data for rat brain was extracted from Goebel and Poosch (1999).

The high expression levels of ccNR2B and ccNR2D resembles that seen in the neonatal rat brain (Monyer et al., 1994). They are relatively diverse in function, whereas NR2B has a high conductance, a high sensitivity to extracellular Mg^{2+} and a relatively short deactivation time, the NR2D has a low conductance, a low sensitivity to extracellular Mg^{2+} and an exceptionally long deactivation time (Dingledine et al., 1999). A study comparing the expression levels of NMDAR subunits in the developing zebrafish nervous system 24-96 hours after fertilization (Cox et al., 2005), detected high levels of NR2A and NR2D and somewhat lower levels of NR2B. Hence, that study agrees with the low levels of NR2C mRNA and the high levels of NR2D mRNA reported in the crucian carp brain.

Remembering that the crucian carp is a tetraploid organism (Raicu et al., 1981), the cloning effort of this study probably missed out on more paralogs than it successfully cloned. Thus, the NR2A-D expression profile presented for crucian carp brain in Figure 11 can only be tentative.

4.5 Phylogenetic Considerations

The crucian carp has proven useful in studying the phenomenon of anoxia tolerance. What seems to be the major advantage for this fish when experiencing anoxia is the ability to transform excess lactate into ethanol excreted over the gills (Figure 1), a feature shared with the goldfish, another species in the genus *Carassius*. Additional features, like the general metabolic depression, the large liver glycogen storage and the upregulation of glycolytic enzymes to run the anaerobic break down of glucose, have enabled these animals to stay conscious and mobile during months of anoxia (Lutz et al., 2003).

WGD events have been hypothesized to increase the number of genes in a lineage (Amores et al., 1998), such as the two WGDs early in vertebrate evolution (Sidow, 1996) and the WGD occurring in ray-finned fish just after their divergence from tetrapods (1-2-4-8 hypothesis, Meyer and Schartl, 1999). Two paralogs were detected for the NMDAR subunits ccNR1, ccNR2A and ccNR2D in crucian carp. These probably origin from a

recent WGD in their evolutionary lineage (Raicu et al., 1981). This WGD would increase the number of genes and make diversity even greater. Indeed, four AMPA receptor subunits have been characterized in mammals (Song and Huganir, 2002), eight have been found in zebrafish, and so far our research group has cloned 12 different subunits in crucian carp. This supports a possible 1-2-4-8-16 hypothesis for crucian carp. A similar scenario must be expected for NMDARs, where a total of four paralogs must be expected for each subunit in crucian carp. Indeed, in zebrafish two paralogs have been identified for each of the genes NR1 and NR2A-D (Figure 7 and 8). The phylogenetic trees in Figure 7 and 8 indicate that these paralogs diverged early in teleost evolution, probably originating from the WGD common to all ray-finned fish (Meyer and Schartl, 1999). The increased diversity come about by such duplications might have played an important role in the evolvement of their anoxia tolerance.

Finally, Figure 9 shows ccNR1.1 and ccNR2A.1-D.1 presented in the same phylogenetic tree. The shared branching points shown by ccNR2A.1 and ccNR2B.1, and by ccNR2C.1 and ccNR2D.1 reflect the functional relationship between the genes (Dingledine et al., 1999). The ccNR1.1 branch leaves the tree between ccNR2C.1 and ccNR2D.1, and not as could have been expected, between ccNR2A.1/ccNR2B.1 and ccNR2C.1/ccNR2D.1. The latter was seen in a zebrafish study by Cox et al. (2005). While the evolutionary analyses of the Cox-study were based on full-length sequences, the analyses of this thesis were based on 500-600 nucleotides. Most likely, the shorter sequences used in this thesis caused the unexpected divergence. Nevertheless, this region proved useful to separately outline the phylogeny of the NR1 and NR2 families.

As previously reported, NMDAR subunits were cloned from red-eared sliders using primers synthesized in this project. These sequences did not always overlap with crucian carp sequences, and with the exeption of NR2A, they could not be included in the phylogenetic analyses presented in Figures 7-8.

5 Conclusion

Crucian carp NMDAR subunit sequences group together with analogous subunits from other vertebrates. It can therefore be concluded that the obtained sequences are NR1, NR2A, NR2B, NR2C and NR2D. The identity of the NR3 family protein was found based on an amino acid BLAST search, and was concluded to be NR3A. Further, two closely related paralogs of the subunits ccNR1, ccNR2A and ccNR2D were identified. This provides evidence for the WGD that has been hypothesized to have taken place in the crucian carp lineage after its divergence from the zebrafish lineage.

The full-length ccNR1 sequence does not display any unique features that could be expected to give this fish a clear advantage in anoxia. Sequence elements representing key functions of the NR1 subunit are well conserved. The alternative cassette 'NTSG' introduced by crucian carp is found in an unresolved, but active area of the rat NR1 protein, and probably function as a N-glycosylation site. This site is probably glycosylated *in vivo*, and may modify NMDAR function, possibly making the receptor better adapted to anoxic conditions.

NR2 subunit composition in crucian carp brain resembles that of embryonic rat brain, where NR2B and NR2D are the major subunits.

Appendices

Appendix I

GenBank Accession Numbers for NMDAR Genes

Gene	Organism	GenBank Accession Number
NR1	Human (*Homo sapiens*)	NM_000832
NR1	Mouse (*Mus musculus*)	BC039157
NR1	Rat (*Rattus norvegicus*)	U08268
NR1 (C1 and C3) [b]	Duck (*Anas platyrhynchus*)	D83352
NR1 (C1 and C3) [b]	Chicken (*Gallus gallus*)	NM_206979
NR1	African clawed frog (*Xenopus laevis*)	X94156
NR1 (C1' and C1'') [a]	Knifefish (*Apteronotus leptorhynchus*)	AF060557
NR1, variant 1	*Tetraodon* (*Tetraodon nigroviridis*)	[c]
NR1, variant 2	*Tetraodon*	[c]
NR1, variant 1 (C1') [a]	Zebrafish (*Danio rerio*)	[c]
NR1, variant 2	Zebrafish	[c]
NR2A	Human	NM_000833
NR2A	Mouse	NM_008170
NR2A	Rat	NM_012573
NR2A	*Takifugu* (*Takifugu rubripes*)	[d]
NR2A variant 1	Zebrafish	[c]
NR2A variant 2	Zebrafish	XM_686662
NR2B	Human	NM_000834
NR2B	Mouse	NM_008171
NR2B	Rat	NM_012574
NR2B	Knifefish	AY166701
NR2B	*Takifugu*	[d]
NR2B variant 1	Zebrafish	XM_683366
NR2B variant 2	Zebrafish	XR_030014
NR2C	Human	NM_000835
NR2C	Mouse	D10694
NR2C	Rat	NM_012575
NR2C	*Tetraodon*	CAG02237
NR2C variant 1	Zebrafish	[c]
NR2C variant 2	Zebrafish	[c]
NR2D	Human	NM_000836
NR2D	Mouse	NM_008172
NR2D	Rat	NM_022797
NR2D	*Takifugu*	[d]
NR2D variant 1	Zebrafish	XM_691632
NR2D variant 2	Zebrafish	XM_001334685
NR3A	Human	AF416558
NR3A	Mouse	AK044171
NR3A	Rat	AF073379
NR3B	Human	NM_138690
NR3B	Mouse	AF396649
NR3B	Rat	NM_133308

[a] For more information on the fish specific C-terminal spleice cassettes C1' and C1'', see (Bottai et al., 1998)
[b] The avian 'C3' splice cassette is called the 'C-terminal variant' in (Kurosawa et al., 1994).
[c] Gene found by performing BLAST search on Ensembl. The genomic sequences found there, were then scanned by GENSCAN to get the exons comprising the gene.
[d] Gene found by performing BLAST search on the FUGU server

Appendix II

Reagents, equipment and software

Reagents

Laboratory kit

Kit Name	**Manufacturer**
BD Advantage™ 2 PCR Kit, 639206	BD Biosciences Clontech
GeneRacer™ Core Kit, L1502-01, Version J	Invitrogen
Genoprep Direct mRNA kit, G316.200	GenoVision
p-GEM®-T Easy Vector Systems, TM042	Promega
Taq Polymerase Kit, 10966-034	Invitrogen
Wizard Plus SV Minipreps DNA Purification System, TB225	Promega

Chemicals

Product, catalog number	**Manufacturer**
Agarose, SeaKem®, 50004	Cambrex
Ampicillin (D[-]-α-Aminobenzylpenicillin), A-9518	Sigma
DEPC (dietyl pyrokarbonat), SD5758	Sigma
DNaseI, D-5307, with 10x Reaction Buffer, R6273	Sigma
dNTP-mix, 10297-018	Invitrogen
Electro competent bacteria E. coli $DH_{5\alpha}$ strain	Invitrogen
Etidium Bromide, 443922U	BDH-Electron
SOC medium, 15544-034	Invitrogen
Superscript II Reverse Transcriptase, 18080-(085)	Invitrogen

Equipment

Product, catalog number / model	**Manufacturer**
Duall glass homogenizer	Kontes
Electroporation cuvette, BTX-610	GeneIronics Inc.
Gene Pulser™ Electroporation machine	BioRad
Eppendorf centrifuge, 5417R	Eppendorf
Finnpipettes, 0,5-10 µl, U23386; 2-20 µl, T27033; 20-200 µl, T27388; 100-1000 µl, T28301	Thermo Labsystems
Mastercycler gradient, 5331	Eppendorf
Spectrophotometer, GeneQuant pro	Amersham Pharmacia Biotech

Software

Software, version	URL/author
BioEdit Sequence Alignment Editor, 7.0.5.3	http://www.mbio.ncsu.edu/BioEdit/page2.html © 1997-2005 by Tom Hall
BLAST (Basic Local Alignment Search Tool)	http://www.ncbi.nlm.nih.gov/BLAST/
ClustalX, 1.83, April 2003	ftp://ftp-igbmc.u-strasbg.fr/pub/ClustalX/
DeepView/Swiss-PdbViewer, v3.7	http://au.expasy.org/spdbv/ © 1995-2001 by Nicolas Guex, Manuel Peitsch, Torsten Schwede and Alexandre Diemand.
GeneDoc Multiple Sequence Alignment Editor & Shading Utility, 2.6.002	http://www.nrbsc.org/gfx/genedoc/index.html © 2000 by Karl Nicholas
GENSCAN	http://genes.mit.edu/GENSCAN.html © 1997-2005 Christopher Burge
LightCycler Probe Design Software, version 1.0	Roche Diagnostics
NetPhos, version 2.0	http://www.cbs.dtu.dk/services/NetPhos/ Center for Biological Sequence Analysis, Technical University of Denmark
NetPhosK Server, version 1.0	http://www.cbs.dtu.dk/services/NetPhosK/ Center for Biological Sequence Analysis, Technical University of Denmark
Phylip, (Phylogeny Inference Package) version 3.6	http://bioweb.pasteur.fr/seqanal/phylogeny/phylip-uk.html © 1986-2004 University of Washington by Joe Felsenstein
Primer3 (Primer Design Software)	http://frodo.wi.mit.edu/cgi-bin/primer3/primer3_www.cgi © 2004 Whitehead Institute for Biomedical Research by Steve Rozen and Helen Skaletsky
Prosite server, release 20.13	http://expasy.org/prosite/ ExPASy Proteomics Server, Swiss Institute of Bioinformatics
SignalP, version 3.0 (Improved prediction of signal peptides)	http://www.cbs.dtu.dk/services/SignalP/ Center for Biological Sequence Analysis, Technical University of Denmark
TMHMM Server, version 2.0	http://www.cbs.dtu.dk/services/TMHMM-2.0/ Center for Biological Sequence Analysis, Technical University of Denmark
TreeView, 1.6.6	http://taxonomy.zoology.gla.ac.uk/rod/treeview.html © 1997 by Roderic D. M. Page

Appendix III

Crucian carp sequences

ccNR1 protein sequence deduced from the mRNA, 905 amino acids

MRLLLLAALFSCSCVRGGCEPKIVNIGAVLSQKRYEQVFKDAVAQANQVYGRD
KFKLTAISVTHKANAIQMALSVCEDLISSQVYAILVSHPPQSTDHLTPTPVSYTAG
FYRIPVVGLTTRMSIYSDKSIHLSFLRTVPPYSHQAHVWFDMMREFRWNHIILIVS
DDHEGRAAQKRLETLLEERETKNKKRNYENQDQLSFDNKRGPKAEKVLQFNQE
TNLTALLLEAKELEARVIILSASEEDAAAVYKTARFLNMTGSGYVWLVGEREMS
GKALSEAPDGLIGLQLINGKNESAHISDAVAVVAQSIQELFEKENITEPPRGCVGN
TNIWKTGPLFKRVLMSSKYPEGLTGRVEFNDDGDRKYAHYSILNYQKSRLLQVG
IYNGTQVVMNKQKKIIWPGGETERPRGFQMSTRLKIVTIHQEPFVYVKPTMLDGT
CKEEYTPNGVLIKKVICTGPNETIPGNTSGRPTVPQCCYGFCVDLLIKLAMTMNFT
YEVHLVADGKFGTQERVNNSNKKEWNGMMGELLGGLADMIVAPLTINNERAQ
YIEFSKPFKYQGLTILVKKEIPRSTLDSFMQPFQSTLWLLVGLSVHVVAVMLYLL
DRFSPFGRFKVNSEEEEEDALTLSSAMWFSWGVLLNSGIGEGAPRSFSARILGMV
WAGFAMIIVASYTANLAAFLVLDRPEERITGINDPMLRNPSDKFIYATVKQSSVDI
YFRRQVELSTMYRHMEKHNYESAAEAIQAVRDNKLHAFIWDSAVLEFEASQKC
DLVTTGGLFFRSGFGIGMRKDSPWKQNVSLAILSSHENGFMEDLDKTWVRYQEC
DSMSNAPATLTFENMAGVFMLVAGGIAAGIFLIFIEIAYKRHKDARGKQMQLAF
AAVNVWRKNLQQFPPTDITGQLNLSDPSVSTVV

ccNR1 mRNA, 4955 bp – CDS from bp 335-3049 marked in blue and real-time RT PCR product highlighted in red

GAGACGCATCACTGATTTTCTGCTGCCAGCTTTCATGCAATATGCGACTTCCT
TGCTCTGCCTGTCTGCAGCCTGACTTAACAGTGGGAATTAAGAGAAAGGCTG
CAGTGAATGCCGCTTCTCTCAGATGCCATCGCCTAGTTGAACCGGGCACCATG
AACAAATCGCCGCAGTGTGTGTGAATTTCGTACCTGGGATATTTTTAAAGTCT
AAAACTGCCACACTGGACATTGCTTTCATTCTTAACAAGCGAATAGCTCAAA
CAAGAGCCTCCGGCAGCACTAAGAAGGGAGGTCACTGGCACTCTCCGTGCGC
TCTTCTGGCCCTCCACACGATGCGTCTGCTTCTGCTGGCCGCGTTGTTCTCCTG

CTCCTGCGTGCGGGGCGGCTGCGAGCCCAAGATTGTGAACATCGGGGCCGTC
CTGAGCCAGAAGAGATACGAGCAGGTGTTCAAGGATGCGGTCGCTCAGGCG
AACCAAGTGTACGGAAGGGATAAATTCAAGTTGACCGCCATCTCTGTCACTC
ACAAAGCTAATGCGATTCAGATGGCACTGTCTGTGTGTGAGGATCTCATTTCC
AGTCAGGTGTATGCCATCCTGGTGAGCCATCCACCACAGTCCACTGACCATCT
GACGCCCACTCCGGTCTCCTACACCGCAGGGTTTTACCGAATACCTGTAGTAG
GGCTTACCACCAGGATGTCCATTTACTCAGACAAGAGCATCCATCTCTCATTC
CTCCGCACAGTGCCACCCTATTCCCACCAGGCACATGTGTGGTTTGACATGAT
GCGGGAGTTCCGCTGGAATCACATCATCCTAATCGTCAGCGATGACCATGAA
GGCAGAGCGGCACAAAAAAGACTAGAAACCCTTCTGGAGGAGAGAGAGACC
AAGAATAAAAAAAGGAACTATGAAAACCAAGACCAACTGTCCTTTGACAAC
AAGAGAGGACCTAAGGCCGAGAAAGTGCTTCAATTCAACCAAGAGACTAAC
TTAACTGCCCTGCTTCTGGAGGCCAAAGAGCTGGAGGCCCGAGTGATCATTC
TCTCTGCCAGTGAGGAAGATGCAGCCGCCGTGTACAAAACAGCACGCTTCCT
CAACATGACAGGCTCAGGCTATGTATGGCTGGTCGGGGAGCGTGAGATGTCC
GGTAAAGCTTTGAGCGAGGCCCCTGATGGGCTGATTGGCCTCCAGCTCATCA
ATGGCAAGAATGAATCGGCGCACATCAGTGATGCCGTTGCTGTCGTAGCCCA
GTCCATCCAAGAGCTCTTTGAGAAAGAGAACATCACAGAACCTCCAAGGGGC
TGCGTGGGCAATACCAACATCTGGAAGACCGGGCCACTTTTTAAAAGGGTAC
TGATGTCTTCCAAGTACCCAGAGGGCCTAACAGGACGCGTTGAGTTCAATGA
TGACGGTGACAGAAAATATGCTCATTACAGCATTCTCAACTACCAGAAGAGC
AGACTGCTTCAAGTCGGCATTTACAATGGAACACAAGTGGTGATGAATAAAC
AGAAGAAGATTATTTGGCCTGGAGGTGAAACAGAAAGACCGAGAGGATTCC
AGATGTCTACTCGATTAAAGATAGTGACCATTCATCAGGAACCCTTTGTGTAT
GTGAAGCCAACTATGCTGGACGGGACCTGCAAGGAAGAGTACACACCTAATG
GAGTCTTAATTAAAAAGGTGATCTGCACTGGACCAAATGAGACCATCCCAGG
TAACACATCAGGACGCCCAACTGTTCCACAATGTTGCTATGGATTTTGCGTTG
ACCTTCTGATCAAATTGGCAATGACCATGAACTTCACCTATGAAGTACACCTG
GTGGCAGATGGGAAATTCGGAACACAAGAAAGGGTAAATAACAGTAACAAG
AAGGAATGGAACGGTATGATGGGTGAGCTCCTGGGTGGCCTTGCTGATATGA
TCGTTGCACCCTTGACAATCAACAATGAACGAGCCCAGTATATAGAATTCTCC

AAGCCTTTCAAATACCAGGGACTAACTATCCTTGTGAAAAAGGAAATTCCTC
GCAGTACACTGGACTCATTCATGCAGCCATTCCAAAGTACACTGTGGCTACTG
GTGGGTTTGTCGGTACATGTGGTGGCGGTGATGCTTTACCTACTAGACCGGTT
CAGCCCTTTTGGAAGGTTTAAAGTAAACAGTGAAGAAGAAGAGGAGGATGC
CCTCACCTTATCTTCAGCTATGTGGTTTTCCTGGGGTGTCTTGTTGAACTCTGG
AATTGGAGAAGGTGCCCCACGTAGTTTTTCAGCAAGAATTTTGGGAATGGTG
TGGGCTGGCTTTGCTATGATTATAGTAGCATCCTATACTGCCAACCTGGCTGC
CTTCCTGGTGTTGGACCGGCCTGAGGAGCGCATCACCGGCATCAATGACCCA
ATGCTAAGGAACCCATCAGACAAGTTCATCTATGCCACAGTGAAGCAAAGTT
CAGTGGATATTTACTTCCGGCGACAAGTTGAGCTGAGCACCATGTACCGCCA
CATGGAGAAGCACAACTACGAAAGCGCCGCTGAAGCCATCCAGGCTGTCCGG
GACAACAAGCTGCATGCTTTCATCTGGGACTCTGCGGTGCTGGAGTTTGAAG
CCTCGCAGAAGTGCGACCTGGTGACCACGGGAGGGCTGTTTTTCCGTTCGGG
CTTTGGCATAGGCATGCGCAAGGACAGCCCCTGGAAACAGAATGTGTCCCTG
GCTATTCTCAGTTCCCATGAGAATGGCTTCATGGAGGACCTAGATAAAACCT
GGGTGAGATACCAGGAGTGTGACTCAATGAGCAATGCCCCAGCCACACTCAC
CTTTGAGAATATGGCAGGTGTCTTCATGCTAGTTGCTGGAGGCATTGCAGCAG
GAATCTTCCTCATCTTCATTGAGATTGCATATAAGCGCCATAAAGACGCCCGC
GGGAAGCAGATGCAGCTAGCCTTTGCGGCCGTCAACGTTTGGAGGAAGAACC
TACAGCAATTCCCACCCACAGACATTACGGGCCAACTCAACTTGTCCGACCC
GTCTGTCAGCACGGTGGTGTGAGGCAGAGAAAGAGGGAGAGTTTAACATAA
AGACAGGCTCATTCTTTAGAGACAAACAAGATGGAACTAGAGAGGAGCATTG
TAGAACCAATCATCTGGACGATGGATCCATCATGGACGAGAACTACTGAGCC
ATTTCACCTTTATGAAGAGCCAGTGGAACCTGTTGGGACTTGATGGTGGACG
GCAGGGGATAGCATGCACTGGAGCACTGCGAACACACAAACCATATAAACA
CATAAACACATACACCTTCATAGCTTGATGCTAAAATAGTATACACTATCATT
CCATCCACCAGAACAACTTCTGAATTAATAATTTATGATTATGTAGAAATATT
TCTTATTAGTATTATCCAAGTACTTATTCTTATGTTGATTAAGTGGTTTAAGTA
TTGTACAGTATAATTTAGAACAAAGAACAAAACTTTTACATGTCTCAAGGCC
AATTCTAAGGCCAGTATTTAGAGAATTAACTAGTTGTATAAGATTAATTATAG
TCATCATTTATATATGATATTTATCTTCTATACATTTTTTATTGTTTTACTTGCT

TTCTGTTCATTGTTTTTCATTCTTTGTCTATATGATCTATAAAGCGAAAAGTCA
GCCAGTCAAGCACATTATCTGCGCTATTTCAATTATCATTATCTTTCATATTCT
AAAATCTCTTTACATATAATATGCATGCAAATTTGTCCCTGAAAGTTTAAGGA
CAAGAAAAAGTATACAGTTAAAATGTTTGATTTAAGATGTGGCTTACTGTAC
ATCAGTTAATTGCAAACTCTCCTTCAAACTCAACTGTTCTTCCTCTTTAAAGTT
CTGACCCAGTCGTTCTCAACTTCAGTCTGAAGGGTGCATCAAGGGGCCGAGT
TTTTTCATCCAACTAGCACTTGGTGTCTCATGCAAAATCATCTCTGTGTGTCGT
CCCCACAGACAACCTCAGAGACCTTTTGCATGAGAAAACCCCAAGTGTGCCC
ATTTATTTTTGACATTGGTGCTGTAGTTTCGTATACACCTATTAGTTGGATGGA
AAAAACTTGCCCGTTCCCAAGTTCTGGGGTTGAGAATCATAAATAAAAGCTG
TACAAATAAGGACTGCTTACTGTAAATGTTCATTTAATGCTATTTATATGACC
CATGGAAAATCCCCTATAAGTGTGATCACCTATAGCACTTTAATGTGAATCTG
TCGGAAGCTATATGCATATGGAAATTATGCAATTTGCCAAATGGTTGATTGTA
ATACTCATACTTGATATGAAAATGCACATTTGAGAATGCGAAATATATTATAT
GTTAATGTCAGCCGTTTGTTTTTTAACAAAACACTCCTTTTGTAGTTTTCTTAT
TTCAAAAGATTTAGACATATTTGTTTCTGATATATATTAGAGTTAAACTGTGT
CAAATTAGTGCATACCACATATATCTTCAGTTTACTACTATTAAGTTACACTA
CTTTAGGTTTTAGTCTTTTAAAACTGACAGGTGTACAGTATGTTTTTTCTCATT
GCTTGAGTCAATGAATGTGGTTTGTACTTAAGAAGAACTATGTATTATATCTG
ATTTCAGGGC-
ATGTAAACACTGAATTCAGTTTATGTTGCCTGGACTGCTAGATTGCAGATGAC
TAAGATGTTGANNNNNNNNNAGGAGTGTTTTTATGAGAAACTGTCACACTGT
TAATACCACACAAACACAATCGGATAAATTACATCACATACAGTAACACACA
TATCCTGAGCATATCCTAAGTGTTACATCATGTTTCAGTTAATTTTAGATATTT
CTCCAAATGAACAAATGTTTGCATTTTGAGAAAAATATATAGAAATAACATT
TATGTTTGCCAATAAATTTGTGCCATGTAAGTTACATACAACAAAAAAAAAA
AAAAAAAAAAAA

ccNR2A, EST, 757 bp, real-time RT PCR product highlighted in red

ACGACTGGCACATCTTCTCGGTGGTCACCACCAAGTTCCCAGGTTTCCAGGAG
TTCATAGCCACCATTCGCGTCACGGTGGACCACAGCTTCATTCGTTGGGACCT

TCAGAGCGTAGTGACGCTGGATGGCGTTGGCGAACCTGAGGACCGTGCCCAC
GTGCAGCTTAAACGCATCCAGTCACCCGTCATCCTCCTCTACTGCTCCAAGGA
CGAAGCGGCATTGGTTATGGAGGAAGCCCGTTCACTAGGGCTCACCGGGGCT
GGCTTTGTGTGGATTGTTCCTGGTCTGACGACAGGAAATCTTGAACAAATCCC
AGAAGCCTTTCCGACTGGGATGATATCTGTGGTGTACGACGAATGGGATTAT
CCCCTGGAGACGCGTGTGCACGACGCTGTGGGAATTATCAGTTCTGCAGCCG
CTGCCATGTTCAGAGAGGAAGGTCGGATACCTGATGGAACGGCTAGCTGCCA
CAGCCAATCAGAGAAGCCGGAAGTGCCGCCAAGTGCTCTGCGAAGATATATG
ATGGGAGTCAGTCTAGGAGGTAGAGATTATTCATTCATGGACGATGGCTACC
AAGTCAATCCCAAGCTGGTCGTCATTGTTCTGAACACACAGAGGGAATGGGA
GAAGATGGGACGATGGGAAAACCACACGTTGAAGTTGAAGTTTCCAGTTTGG
CCACGTTATAACTCATTTGGGGACATGGACGCTGATGAGAACCACTTGAGCA
TTGTGACTCTAGAGGAAAGACCCTT

ccNR2B, EST, 968 bp, real-time RT PCR product highlighted in red

AAGAAGCTGCAGAGCCCCGTCATCCTGCTCTACTCCACCAAAGAGGAGGCCA
ACATCATCTTCCAGGTGGCACACTCTGTGGGCCTGACGGGCTACGGCTACAC
CTGGATCGCCCCGTCTCTGGTGGCAGGAGACGCCGACCACATCCCGGCCGAG
TTCCCCACAGGCATGATCTCAGTGTCGTACGACGAGTGGGATTACGGTCTGG
AGGCACGCGTTCGTGACGGTGTGGCTGTGATCGCCTCGGCCACCTCCACCAT
GATGATAGAACGAGGGCCACACACACTGCTCAAGTCTGAGTGCCACGGGGCC
CCGGACAAGAAGAGCCCCATCAGCAACGAGGTGCTCAGGTATCTGATGAACG
TGACGTTCGAGGGCCGGAATCTCTCCTTCAGTGAGGACGGCTATCAGATGCA
CCCCAAACTGGTGATCATCCTGCTGAACAAGGACAGACAGTGGGACAGAGTG
GGTAAGTGGGAGAACGGCTCTCTGTCGATGAAGTTTCACGTGTGGCCGCGGT
TCGAGCTCTACTCTGGGACGGAGAGCCGAGAGGACGATCATCTGTCCATCGT
GACGCTGGAGGAGGCTCCGTTCGTGATGGTGGAGGACGTGGATCCACTCAGC
GGCACCTGCATGAGGAACACGGTTCCCTGCCGCAAGCAGCTCAAAACACTGA
ATAAGACGGGGGATTCTGGCATCTACATCAAGCGCTGCTGTAAAGGCTTCTG
TATCGACATCCTGAAGAAGATCGCCAAGTCTGTGAAGTTCACCTACGACCTTT
ATCTGGTCACCAATGGCAAACACGGCAAGAAGATCAACGGCACATGGAATG

GGATGGTGGGAGAGGTGGTGCTGAAGAACGCTCACATGGCTGTTGGCTCGCT
GACCATCAATGAGGAGAGGTCAGAGGTCATTGATTTCTCCGTGCCCTTCATA
GAGACAGGCATCAGTGTTATGGTGTCTCGCAG

ccNR2C, EST, 788 bp, real-time RT PCR product highlighted in red

GTACAACTGGGGCAACTTTGTGGTGATCACCAGCTTGTATCCCGGCTACGAG
ACCTTCTTGGACTACATCCGCTCCTTCACAGACACCAGCTACTTCCTGTGGGA
GCTGCGGGATGTGCTGAGCTTTGAGATGTCTGTGGGGGCCAATGACATCCGC
ACAAGAAGACTACTACAGCAGGTGGACTCGCAGGTATACCTAGTGTACTGTT
CCCATGAGGAGGCACAGTACTTGTTCAGGATGGCCTCTGATGTGGGGCTTCT
AGGGCCCGGATACATCTGGGTCATCCCCAGCCTGGCTGTGGGGAACCCTGAA
GTGTCCCCTCCTGACAGTTTCCCTGTGGGCGTCATCAGTATTATCACAGACCG
CTGGAGGAAAACACTGCGCCAGAGGGTTCGGGAAGGAGTCGCAGTCATAGT
AAAAGGGGTGCACAGCTTTTATAAGAACAGAGGATTCATTCCCGATGGTCAC
AGTGACTGCAATAGTCCTGTCAAATCGTACGCCAACAATTCTCTCTTCAGGCA
TATGCTAAATGTGTCATGGGAGCATAAGGACCTCTCCTTCAACACTGATGGCT
ATCTCACCAATCCTTCCATGGTGATCATTGCTTTGGATCGAGAGAGACACTGG
GACAAGGTAGGAAGCTACGAGGGAGGGATTCTGCAGATGCGATACCCTGTAT
GGCCCCGTTACGGCAGCTTCCTGGAGCCCGTGTCTGACAACCGGCACCTGAC
TGTGGCCACGCTGGAGGAGAGGCCTTTTGTCATCGTAGAGAGTGTTGATCCT
GCCA

ccNR2D, EST, 1132 bp, real-time RT PCR product highlighted in red

TTGAGGTGCTGGAGGAGTACGATTGGACGGCCTTCTCGGTGGTGTCCACACG
TCACCATGGCTACCAGGACTTCCTGTCAGTAGTGGAAGGTTTGACCGACGGG
TCATTCATCGGCTGGGAGAAGAAGAGCGTAGTGATGTTGAATTTAACCGATG
ACCCAGGAGGAGCACGTGCACGACGGCTACTGAAAGAGAATGAAGCACAGG
TGCGGTTGTTGTACTGCTCTCAAGAGGAAGCAGAACAGGTGTTCCACGCTGC
TTGGGCAGCTGGTCAGGCCAGTGCCTCTCACATATGGTTCGCGGTGGGTCCG
GCTCTGTCAGAGCTGGGCCTGACCGGACTTCCCAATCGACTGTTTGCGGTCAG
ACCGCAGGGCTGGAGGGACGAACCCCGCCGTCGTATCGCCCGTGGGGTGTCC
ATCCTTACCCATGGAGCGGTCGCGTTGCGGAAAGACTATGGAGCCACTGGAG

GCCCTCACTTTGTCACTAACTGCCAGACAGAAGGCAACGGAACACAGAGGAT
TCGCGGTAGAATGAAGTATTTCAGTAACATCACACTCGGTGGGCGGGACTAT
TCGTTCAATAATGAGGGCTACCTGGCCAACCCCTTTCTGGATGTCATCTCCTA
CACGTCTGGGAGTGGCTGGGAAGACGTGGGATGGTGGGAGAACGGGGTGTT
ACGTCTGAGGTATCCTGCTTGGTCTAGATATAGCCCCTTCCTGCAGCCGCCCG
ATGATGCTCAGCACCTGAGGGTCGTGACCCTGGAGGAGCGGNCCTTCGTTAT
CGTGGAGCTAGCAGACCCTTCCTCTGGAACCTGCATTAGGGACTCCGTGCCAT
GCAGACGGCCTCTCAATGCCAGTGCACTTCAAGAAGGGGTGGCACCTATGAA
ACAGTGCTGCAAAGGATTCTGCATCGACATCCTTAAGCGACTGGCCAGAATT
GTCGGCTTTACCTATGACCTCTACTTGGTGACCAATGGGAAACATGGAAAAA
AGATTGATGGAGTTTGGAACGGGATGGTGGGAGAGGTTGTGTACAAGCGGGC
AGACATGGCGATCGGCTCTCTCACTATCAACGAGGAGAGGTCAGAGGTCGTG
GACTTCTCTGTGCCCTTTGTGGAGACAGGCATCAGCGTT

ccNR3A, EST, 283 bp, real-time RT PCR product highlighted in red

TGTACATAGTTGGGGACGGGAAATATGGAGCTGTCAAGGGTGGACAGTGGAC
AGGGTTGGTGGGTGACCTGCTGAGCGGGGTGGCCGATATGGCTGTTACCAGC
TTCAGCATCAATTCAGCTCGCAGTAAAGTGATTGACTTCACCAGCCCGTTCTT
TTCCACGAGTTTGGGCATACTTGTGCGCAGTAAGGACACGGCGGCACCAATC
GGAGCGTTCATGTGGCCGTTGCACTGGTCCATGTGGATGGGCATCTTTGTGGC
GCTGCACATCACAGCGCTCTT

References

Al-Hallaq, R. A., Jarabek, B. R., Fu, Z., Vicini, S., Wolfe, B. B. and Yasuda, R. P. (2002). Association of NR3A with the N-methyl-D-aspartate receptor NR1 and NR2 subunits. *Mol Pharmacol* **62**, 1119-27.

Amores, A., Force, A., Yan, Y. L., Joly, L., Amemiya, C., Fritz, A., Ho, R. K., Langeland, J., Prince, V., Wang, Y. L. et al. (1998). Zebrafish hox clusters and vertebrate genome evolution. *Science* **282**, 1711-4.

Andersson, O., Stenqvist, A., Attersand, A. and von Euler, G. (2001). Nucleotide sequence, genomic organization, and chromosomal localization of genes encoding the human NMDA receptor subunits NR3A and NR3B. *Genomics* **78**, 178-84.

Bickler, P. E., Donohoe, P. H. and Buck, L. T. (2000). Hypoxia-induced silencing of NMDA receptors in turtle neurons. *J Neurosci* **20**, 3522-8.

Bottai, D., Maler, L. and Dunn, R. J. (1998). Alternative RNA splicing of the NMDA receptor NR1 mRNA in the neurons of the teleost electrosensory system. *J Neurosci* **18**, 5191-202.

Buck, L. T. and Bickler, P. E. (1998). Adenosine and anoxia reduce N-methyl-D-aspartate receptor open probability in turtle cerebrocortex. *J Exp Biol* **201 (Pt 2)**, 289-97.

Chatterton, J. E., Awobuluyi, M., Premkumar, L. S., Takahashi, H., Talantova, M., Shin, Y., Cui, J., Tu, S., Sevarino, K. A., Nakanishi, N. et al. (2002). Excitatory glycine receptors containing the NR3 family of NMDA receptor subunits. *Nature* **415**, 793-8.

Chazot, P. L. and Stephenson, F. A. (1997). Biochemical evidence for the existence of a pool of unassembled C2 exon-containing NR1 subunits of the mammalian forebrain NMDA receptor. *J Neurochem* **68**, 507-16.

Chen, P. E. and Wyllie, D. J. (2006). Pharmacological insights obtained from structure-function studies of ionotropic glutamate receptors. *Br J Pharmacol* **147**, 839-53.

Ciabarra, A. M., Sullivan, J. M., Gahn, L. G., Pecht, G., Heinemann, S. and Sevarino, K. A. (1995). Cloning and characterization of chi-1: a developmentally regulated member of a novel class of the ionotropic glutamate receptor family. *J Neurosci* **15**, 6498-508.

Conn, P. J. and Pin, J. P. (1997). Pharmacology and functions of metabotropic glutamate receptors. *Annu Rev Pharmacol Toxicol* **37**, 205-37.

Cox, J. A., Kucenas, S. and Voigt, M. M. (2005). Molecular characterization and embryonic expression of the family of N-methyl-D-aspartate receptor subunit genes in the zebrafish. *Developmental Dynamics* **234**, 756-766.

Cull-Candy, S., Brickley, S. and Farrant, M. (2001). NMDA receptor subunits: diversity, development and disease. *Curr Opin Neurobiol* **11**, 327-35.

Cull-Candy, S. G. and Leszkiewicz, D. N. (2004). Role of distinct NMDA receptor subtypes at central synapses. *Sci STKE* **2004**, re16.

Curtis, D. R., Phillis, J. W. and Watkins, J. C. (1959). Chemical excitation of spinal neurones. *Nature* **183**, 611-2.

Dingledine, R., Borges, K., Bowie, D. and Traynelis, S. F. (1999). The glutamate receptor ion channels. *Pharmacol Rev* **51**, 7-61.

Don, R. H., Cox, P. T., Wainwright, B. J., Baker, K. and Mattick, J. S. (1991). Touchdown Pcr to Circumvent Spurious Priming During Gene Amplification. *Nucleic Acids Res* **19**, 4008-4008.

Ehlers, M. D., Zhang, S., Bernhadt, J. P. and Huganir, R. L. (1996). Inactivation of NMDA receptors by direct interaction of calmodulin with the NR1 subunit. *Cell* **84**, 745-55.

Force, A., Lynch, M., Pickett, F. B., Amores, A., Yan, Y. L. and Postlethwait, J. (1999). Preservation of duplicate genes by complementary, degenerative mutations. *Genetics* **151**, 1531-45.

Furukawa, H. and Gouaux, E. (2003). Mechanisms of activation, inhibition and specificity: crystal structures of the NMDA receptor NR1 ligand-binding core. *Embo J* **22**, 2873-85.

Goebel, D. J. and Poosch, M. S. (1999). NMDA receptor subunit gene expression in the rat brain: a quantitative analysis of endogenous mRNA levels of NR1Com, NR2A, NR2B, NR2C, NR2D and NR3A. *Brain Res Mol Brain Res* **69**, 164-70.

Hall, T. A. (1999). BioEdit: a user-friendly biological sequence alignment editor and analysis program for Windows 95/98/NT. *Nucl. Acids. Symp. Ser.* **41**, 95-98.

Hollmann, M. and Heinemann, S. (1994). Cloned glutamate receptors. *Annu Rev Neurosci* **17**, 31-108.

Hyvärinen, H., Holopainen, I. J. and Piironen, J. (1985). Anaerobic wintering of crucian carp (*Carassius carassius* L.) - 1. Annual dynamics of glycogen reserves in nature. *Comp Biochem Physiol A* **82A**, 797-803.

Ikeda, K., Nagasawa, M., Mori, H., Araki, K., Sakimura, K., Watanabe, M., Inoue, Y. and Mishina, M. (1992). Cloning and expression of the epsilon 4 subunit of the NMDA receptor channel. *FEBS Lett* **313**, 34-8.

Ishii, T., Moriyoshi, K., Sugihara, H., Sakurada, K., Kadotani, H., Yokoi, M., Akazawa, C., Shigemoto, R., Mizuno, N., Masu, M. et al. (1993). Molecular characterization of the family of the N-methyl-D-aspartate receptor subunits. *J Biol Chem* **268**, 2836-43.

Jackson, D. C. (2000). How a Turtle's Shell Helps It Survive Prolonged Anoxic Acidosis. *News Physiol Sci* **15**, 181-185.

Johansson, D., Nilsson, G. E. and Doving, K. B. (1997). Anoxic depression of light-evoked potentials in retina and optic tectum of crucian carp. *Neurosci Lett* **237**, 73-6.

Johnston, I. A. and Bernard, L. M. (1983). Utilization of the ethanol pathway in carp following exposure to anoxia. *J Exp Biol* **104**, 73-78.

Kornau, H. C., Schenker, L. T., Kennedy, M. B. and Seeburg, P. H. (1995). Domain Interaction between Nmda Receptor Subunits and the Postsynaptic Density Protein Psd-95. *Science* **269**, 1737-1740.

Kurosawa, N., Kondo, K., Kimura, N., Ikeda, T. and Tsukada, Y. (1994). Molecular cloning and characterization of avian N-methyl-D-aspartate receptor type 1 (NMDA-R1) gene. *Neurochem Res* **19**, 575-80.

Kutsuwada, T., Kashiwabuchi, N., Mori, H., Sakimura, K., Kushiya, E., Araki, K., Meguro, H., Masaki, H., Kumanishi, T., Arakawa, M. et al. (1992). Molecular diversity of the NMDA receptor channel. *Nature* **358**, 36-41.

Leggatt, R. A. and Iwama, G. K. (2003). Occurrence of polyploidy in the fishes. *Reviews in Fish Biology and Fisheries* **13**, 237-246.

Lipton, P. (1999). Ischemic cell death in brain neurons. *Physiol Rev* **79**, 1431-568.

Lutz, P. L., Nilsson, G. E. and Prentice, H. (2003). The Brain Without Oxygen: Causes of Failure - Molecular and Physiological Mechanisms for Survival. Dordrecht, The Netherlands: Kluwer Academic Publishers.

McBain, C. J. and Mayer, M. L. (1994). N-methyl-D-aspartic acid receptor structure and function. *Physiol Rev* **74**, 723-60.

McFeeters, R. L. and Oswald, R. E. (2004). Emerging structural explanations of ionotropic glutamate receptor function. *Faseb J* **18**, 428-38.

Meguro, H., Mori, H., Araki, K., Kushiya, E., Kutsuwada, T., Yamazaki, M., Kumanishi, T., Arakawa, M., Sakimura, K. and Mishina, M. (1992). Functional characterization of a heteromeric NMDA receptor channel expressed from cloned cDNAs. *Nature* **357**, 70-4.

Meyer, A. and Schartl, M. (1999). Gene and genome duplications in vertebrates: the one-to-four (-to-eight in fish) rule and the evolution of novel gene functions. *Curr Opin Cell Biol* **11**, 699-704.

Monyer, H., Burnashev, N., Laurie, D. J., Sakmann, B. and Seeburg, P. H. (1994). Developmental and regional expression in the rat brain and functional properties of four NMDA receptors. *Neuron* **12**, 529-40.

Monyer, H., Sprengel, R., Schoepfer, R., Herb, A., Higuchi, M., Lomeli, H., Burnashev, N., Sakmann, B. and Seeburg, P. H. (1992). Heteromeric NMDA receptors: molecular and functional distinction of subtypes. *Science* **256**, 1217-21.

Moriyoshi, K., Masu, M., Ishii, T., Shigemoto, R., Mizuno, N. and Nakanishi, S. (1991). Molecular cloning and characterization of the rat NMDA receptor. *Nature* **354**, 31-7.

Nicholas, K. B. and Nicholas, H. B. J. (1997). GeneDoc: a tool for editing and annotating multiple sequence alignments.

Nicoll, R. A. (2003). Expression mechanisms underlying long-term potentiation: a postsynaptic view. *Philos Trans R Soc Lond B Biol Sci* **358**, 721-6.

Nilsson, G. E. (1990). Long-term anoxia in crucian carp: changes in the levels of amino acid and monoamine neurotransmitters in the brain, catecholamines in chromaffin tissue, and liver glycogen. *J Exp Biol* **150**, 295-320.

Nilsson, G. E. and Renshaw, G. M. (2004). Hypoxic survival strategies in two fishes: extreme anoxia tolerance in the North European crucian carp and natural hypoxic preconditioning in a coral-reef shark. *J Exp Biol* **207**, 3131-9.

Nilsson, G. E., Rosén, P. and Johansson, D. (1993). Anoxic depression of spontaneous locomotor activity in crucian carp quantified by a computer imaging technique. *J Exp Biol*, 153-162.

Nishi, M., Hinds, H., Lu, H. P., Kawata, M. and Hayashi, Y. (2001). Motoneuron-specific expression of NR3B, a novel NMDA-type glutamate receptor subunit that works in a dominant-negative manner. *J Neurosci* **21**, RC185.

Perez-Otano, I., Schulteis, C. T., Contractor, A., Lipton, S. A., Trimmer, J. S., Sucher, N. J. and Heinemann, S. F. (2001). Assembly with the NR1 subunit is

required for surface expression of NR3A-containing NMDA receptors. *J Neurosci* **21**, 1228-37.

Premkumar, L. S. and Auerbach, A. (1997). Stoichiometry of recombinant N-methyl-D-aspartate receptor channels inferred from single-channel current patterns. *J Gen Physiol* **110**, 485-502.

Raicu, P., Taisescu, E. and Banarescu, P. (1981). Carassius-Carassius and Carassius-Auratus, a Pair of Diploid and Tetraploid Representative Species (Pisces, Cyprinidae). *Cytologia* **46**, 233-240.

Rees, B. B., Sudradjat, F. A. and Love, J. W. (2001). Acclimation to hypoxia increases survival time of zebrafish, Danio rerio, during lethal hypoxia. *J Exp Zool* **289**, 266-72.

Roesner, A., Hankeln, T. and Burmester, T. (2006). Hypoxia induces a complex response of globin expression in zebrafish (Danio rerio). *J Exp Biol* **209**, 2129-37.

Shoubridge, E. A. and Hochachka, P. W. (1980). Ethanol: novel end product of vertebrate anaerobic metabolism. *Science* **209**, 308-9.

Sidow, A. (1996). Gen(om)e duplications in the evolution of early vertebrates. *Curr Opin Genet Dev* **6**, 715-22.

Sitbon, E. and Pietrokovski, S. (2007). Occurrence of protein structure elements in conserved sequence regions. *BMC Struct Biol* **7**, 3.

Song, I. and Huganir, R. L. (2002). Regulation of AMPA receptors during synaptic plasticity. *Trends Neurosci* **25**, 578-588.

Standley, S. and Baudry, M. (2000). The role of glycosylation in ionotropic glutamate receptor ligand binding, function, and trafficking. *Cell Mol Life Sci* **57**, 1508-16.

Standley, S., Roche, K. W., McCallum, J., Sans, N. and Wenthold, R. J. (2000). PDZ domain suppression of an ER retention signal in NMDA receptor NR1 splice variants. *Neuron* **28**, 887-98.

Storey, K. B. (1987). Tissue-specific controls on carbohydrate catabolism during anoxia in goldfish. *Physiological Zoology* **60**, 601-607.

Sucher, N. J., Akbarian, S., Chi, C. L., Leclerc, C. L., Awobuluyi, M., Deitcher, D. L., Wu, M. K., Yuan, J. P., Jones, E. G. and Lipton, S. A. (1995). Developmental and regional expression pattern of a novel NMDA receptor-like subunit (NMDAR-L) in the rodent brain. *J Neurosci* **15**, 6509-20.

Szatkowski, M. and Attwell, D. (1994). Triggering and execution of neuronal death in brain ischaemia: two phases of glutamate release by different mechanisms. *Trends Neurosci* **17**, 359-65.

Taylor, J. S., Braasch, I., Frickey, T., Meyer, A. and Van de Peer, Y. (2003). Genome duplication, a trait shared by 22000 species of ray-finned fish. *Genome Res* **13**, 382-90.

Taylor, J. S., Van de Peer, Y., Braasch, I. and Meyer, A. (2001). Comparative genomics provides evidence for an ancient genome duplication event in fish. *Philos Trans R Soc Lond B Biol Sci* **356**, 1661-79.

Thompson, J. D., Gibson, T. J., Plewniak, F., Jeanmougin, F. and Higgins, D. G. (1997). The CLUSTAL_X windows interface: flexible strategies for multiple sequence alignment aided by quality analysis tools. *Nucleic Acids Res* **25**, 4876-82.

Traynelis, S. F., Hartley, M. and Heinemann, S. F. (1995). Control of proton sensitivity of the NMDA receptor by RNA splicing and polyamines. *Science* **268**, 873-6.

Tzeng, D. W., Lin, M. H., Chen, B. Y., Chen, Y. C., Chang, Y. C. and Chow, W. Y. (2007). Molecular and functional studies of tilapia (Oreochromis mossambicus) NMDA receptor NR1 subunits. *Comp Biochem Physiol B Biochem Mol Biol* **146**, 402-11.

Val, A. L., Silva, M. N. P. and Almeida-Val, V. M. F. (1998). Hypoxia adaptation in fish of the Amazon: a never-ending task. *South African Journal of Zoology* **33**, 107-114.

Vandenberghe, W. and Bredt, D. S. (2004). Early events in glutamate receptor trafficking. *Curr Opin Cell Biol* **16**, 134-9.

Volff, J. N. (2005). Genome evolution and biodiversity in teleost fish. *Heredity* **94**, 280-94.

Wissing, J. and Zebe, E. (1988). The Anaerobic Metabolism of the Bitterling Rhodeus-Amarus (Cyprinidae, Teleostei). *Comparative Biochemistry and Physiology B-Biochemistry & Molecular Biology* **89**, 299-303.

Yamazaki, M., Mori, H., Araki, K., Mori, K. J. and Mishina, M. (1992). Cloning, expression and modulation of a mouse NMDA receptor subunit. *FEBS Lett* **300**, 39-45.

Zheng, X., Zhang, L., Durand, G. M., Bennett, M. V. and Zukin, R. S. (1994). Mutagenesis rescues spermine and Zn2+ potentiation of recombinant NMDA receptors. *Neuron* **12**, 811-8.

Zukin, R. S. and Bennett, M. V. (1995). Alternatively spliced isoforms of the NMDARI receptor subunit. *Trends Neurosci* **18**, 306-13.